APPENDIX A: A REFERENCE MANUAL ON THE THEORY AND NUMERICAL METHODS UNDERLYING THE WIPP CODE CUTTINGS_S (BY J. W. BERGLUND)

This appendix describes the theoretical basis of the CUTTINGS_S computer code which was written to calculate the quantity of solid radioactive material (in curies) brought to the surface from a radioactive waste disposal facility as a consequence of an inadvertent drilling intrusion. The code determines the amount of material removed by several release mechanisms, and decays the releases to the intrusion time. The report describes the background, assumptions, equations, and variables governing the releases and the methods used to solve them. The code was written specifically for the computations required for the Performance Assessment of the Waste Isolation Pilot Project (WIPP) but with due care can be used for other radioactive waste repositories.

1.0 Introduction

The Waste Isolation Pilot Plant (WIPP), located in southern New Mexico, is the first planned, mined geologic repository for transuranic wastes generated by U.S. defense programs. WIPP is currently being evaluated to assess compliance with the requirements of EPA 40 CFR 191 Subpart B. Briefly, this requirement, promulgated by the Environmental Protection Agency, limits the amount of radioactive material that can be released to the accessible environment over a 10,000-year regulatory period.

Of the possible pathways for release during this period, one of the most important is that caused by the inadvertent penetration of a waste storage room by an exploratory drill bit. The current performance assessment model relies on the assumption that future drilling techniques will be similar to those in use today. The validity of this assumption is unknown but is necessary to provide a basis on which predictions of release can be estimated. Assuming that current, standard drilling practices for gas and oil are used, mechanisms governing the direct removal of radioactive waste can be identified and governing equations developed and solved. The following report summarizes the current understanding of the processes related to the direct removal of wastes, presents the governing mechanisms, and describes the solution of the model equations.

1.1 Background

The WIPP repository will consist of a number of excavated waste disposal rooms located in bedded halite (salt) approximately 650m below the ground surface in southeast New Mexico. Most excavated rooms will be approximately 91 m long, 10 m wide and 4 m high. Transuranic waste packaged in 55-gallon drums or standard waste boxes will be placed in each room and backfilled primarily with crushed salt.

After the WIPP repository is filled with waste and sealed, the waste is expected to be slowly compacted vertically by salt creep from an original waste room height of 4 m to a compacted height of 0.5 to 2 m within 100 to 200 years. The overburden (vertical) stress acting on the waste will also increase to the lithostatic stress (~14.8 MPa) during this period. The waste in its unmodified form will consist of a mixture of contaminated organic (e.g., cloth, wood, rubber, plastics) and inorganic (e.g. metals, glass) materials. After placement in the mined (salt) repository, the waste will be compacted by creep closure of the surrounding salt and in addition may become exposed to brine. The exposure of the metallic waste to brine is expected to cause corrosion of the metals and as a by-product will generate gas (H_2). Additional gas will be generated by the biodegradation of the organic materials in the waste inventory. The gas volumes

generated by corrosion and biodegradation are expected to increase continuously for hundreds of years and the pore pressure may reach and possibly exceed the lithostatic overburden stress. During this time the repository is also expected to expand under the influence of the elevated gas pressure.

At some time within the 10,000-year regulatory period, it is probable that one or more exploration boreholes will be drilled into and through the vertically compacted waste and some of the waste will be carried to the surface as a direct result of the drilling process. The volume of waste removed to the ground surface will depend upon the physical properties of the compacted, decomposed wastes, the drilling procedures used, and the pore pressures encountered. Because of radioactive decay, the radioactivity of nuclides in the removed waste (in curies) will also depend upon the time of intrusion.

1.2 Current Drilling Practices

In considering the problem of the direct releases caused by drilling it is important to understand the procedures currently utilized in drilling a gas or oil well. The following description is tailored to practices in use near the WIPP site. Typically, independent drilling companies respond to requests for fixed price bids from oil companies to provide drilled and cased holes of a specified diameter to a specified depth at a location leased by the oil company. The bids are competitive and generally the low bidder is selected. As a result of this bidding process, profit margins for the winning driller are governed by the effectiveness of the driller in maintaining efficient drilling parameters and by solving unforeseen difficulties that may arise quickly and safely. The principal goal of the driller is to "make hole" and meet contract requirements. If this is accomplished the drilling operation will be profitable.

Within the Delaware Basin near the WIPP site, gas and oil wells are started by clearing the site, and drilling a shallow hole (~40') to house a conductor pipe. The conductor pipe is set in cement and serves to prevent surface sands from sloughing into the wellbore during later drilling. Below the conductor, drilling is continued to 300 - 600 feet (to top of salt section) using a large diameter (17-26") drill bit and another steel casing is set. This "surface" casing is cement grouted into the hole and a blowout preventer tree is attached to the casing at the surface. Drilling below the surface casing (in the salt section) uses a drilling mud that consists of a saturated brine solution to prevent dissolution of the salt. Drilling through the salt section proceeds at rates from 50 to 100 feet/hour depending on bit diameter. If higher rates are attempted by increasing the weight on bit (WOB) there is the danger of producing a crooked hole. While in the salt section, drilling mud (brine) is supplied from a large plastic lined reserve pit dug in the ground with a surface area of approximately 4000 ft^2. Drilling mud is pumped from the reserve pit down through the drillpipe and drillbit and up the annulus formed by the drillstring and drilled hole. The drilling mud and drill cuttings are returned directly to the reserve pit where the cuttings settle out. While drilling in the salt section no formal attempt is made to monitor the character of the cuttings or the fluid volume of the reserve pit. A gas analyzer is not attached to the returns until the hole is much deeper than the depth of the WIPP repository. The drillstring generally consists of a drillbit attached to approximately 20, 30 foot long drill collars followed by multiple sections of 30 foot long 4 1/2 " diameter drillpipe. One to four drillbit changes may be necessary when drilling through the salt section. This process requires the removal of the entire drillstring (tripping). Once the drill has passed the salt section (~4500 ft) the hole is again cased and set with cement. At this point, if the repository had been penetrated no further contact would occur between the drilling mud and the exposed WIPP waste.

2.0 Release Processes

Three separate physical processes are assumed to influence the quantity of waste brought to the ground surface as the result of the inadvertent penetration of the repository by an exploratory drill bit. These are:

*Cuttings - waste contained in the cylindrical volume created by the cutting action of the drill bit passing through the waste.

*Cavings - waste that erodes from the borehole in response to the upward-flowing drilling fluid within the annulus, and

*Spallings - waste introduced into the drilling fluid caused by the release of waste-generated gas escaping to the lower-pressure borehole. This requires a repository gas pressure that exceeds the hydrostatic pressure of the drilling mud.

In the above and in the following it is understood that usage of the word "waste" also includes any backfill or other materials that may have been added to the actual waste material.

Spallings can be further subdivided into three regimes that are dependent upon the state of waste permeability and gas pore pressure at the time of intrusion. These are:

**Blowout - the direct release of waste to the surface in waste decomposition gas that has cleared the borehole annulus of drilling mud and is flowing freely to the surface.

**Gas Erosion - low permeability waste that is pressed against the drillstring due to stresses from escaping decomposition gas and is eroded by the flowing drilling mud.

**Stuck Pipe - low permeability waste that is pressed against the drillstring sufficiently hard to prevent normal drilling. This occurs at high gas pressures.

These release processes and when they are active are depicted graphically in Figure 1.

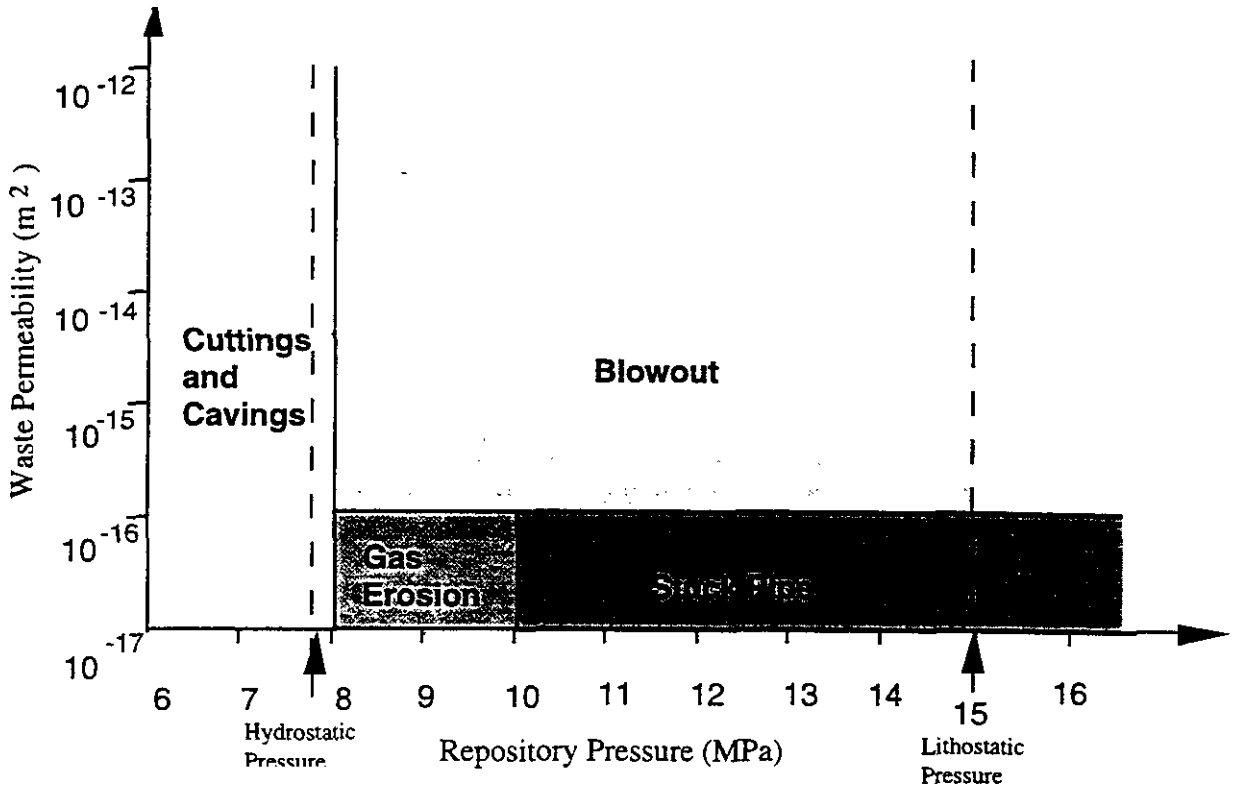

Figure 1. Release process zones

The release process zone boundaries are based on waste permeability and repository gas pressure and will be discussed in the model descriptions for the zones. Detailed descriptions of the release process zones, their principal assumptions, and mathematical formulation will be discussed in the following sections.

2.1 Cuttings

This is the simplest component of the direct release model and is assumed to occur for repository pressures less than the hydrostatic pressure of the drilling mud. This pressure is approximately 8 Mpa (Figure 1). For a gauge borehole, the volume of cuttings removed and transported to the surface is equal to the product of the drill bit area and the drill depth. Thus, to estimate the total solid volume of waste removed due to the cutting action of the drill bit , it is only necessary to know the compacted repository height (H), the porosity at the time of intrusion (φ), and the drill bit area (A).

$$Volume = AH(1-\varphi) \tag{1}$$

The cuttings volume calculated in this manner is a lower bound to the total quantity of waste removed by drilling. In the CUTTINGS_S code the waste is assumed to be uniformly distributed throughout the disposal region. Thus the actual computation for release requires only the drill bit area and the waste curie content per unit area. The actual computation of cuttings release in the CUTTINGS_S code is computed within the module for cavings. This description follows.

2.2 Cavings

The cavings component of direct surface release consists of that quantity of waste material that is eroded from the borehole wall by the action of the flowing drilling fluid after a waste disposal room is penetrated. The erosion process is assumed to be driven solely by the shearing action of the drilling fluid (mud) on the waste as it moves up the borehole annulus. For cavings it is further assumed that the repository is not pressurized by either brine or gas, i.e. the repository pressure is less than the hydrostatic pressure caused by a brine column to the surface (Figure 1). Gas pressurization effects are included in other release processes (spall) and will be discussed later.

In the annulus formed by the collars or drill pipe and the borehole wall, the flow of the drilling fluid has both a vertical and rotational component. Within this helical flow pattern, shear stresses are generated by the relative motion of adjacent fluid regions and by the action of the fluid on the borehole wall. In this model, it is assumed that if the fluid shear stress at the wall exceeds the effective shear resistance to erosion of the wall material (compacted repository wastes), erosion of the wall material will occur, increasing the diameter of the bored hole. The eroded material will then be passed to the surface in the flowing drilling fluid.

Flow in the annulus between the drillpipe and borehole wall is usually laminar (Darley and Gray, 1988, p243). Adjacent to the collars, however, the flow may be either laminar or turbulent as a consequence of the larger collar diameter and resulting higher mud velocities. For laminar flow, the analysis lends itself to classical solution methods. Turbulent flow, where the flow is assumed to be axial with a correction for the rotational component, requires a more approximate approach. A discussion of these two cases follows.

2.2.1 Laminar Flow

Below Reynolds numbers of about 2100 for Newtonian fluids and 2400 for some non-Newtonian fluids (Walker, 1976), experiments have shown that the flow of a fluid in a circular pipe or annulus is well behaved and can be described using a well-defined relationship between the velocity field and the fluid shear stress. This type of flow is called laminar.
Some of the early work on laminar helical flow of a non-Newtonian fluid in an annulus was performed by Coleman and Noll (1959), and Fredrickson (1960). The laminar helical flow solution procedure outlined below and used in the CUTTINGS_S code is, for the most part, an adaptation of methods described in a paper by Savins and Wallick (1966).

One of the principal difficulties in solving for the shear stresses within a helically flowing drilling fluid is the shear rate dependence of the fluid viscosity. This non-Newtonian fluid behavior necessitates choosing a functional form for the variation of viscosity with shear rate for the fluid. There are several functional forms for the viscosity of drilling fluids that can be assumed. For example, in the oil and gas industry the Bingham and power law models are often used to approximate the shear rate dependence of the fluid viscosity. A less common function is a form chosen by Oldroyd (1958) and used in the analysis by Savins and Wallick (1966). Oldroyd assumed that the viscosity varied according to the functional relation

$$\eta = \eta_o \left[\frac{1 + \sigma_2 \Gamma^2}{1 + \sigma_1 \Gamma^2} \right] \qquad (2)$$

where σ_1 and σ_2 are constants, η_o is the limiting viscosity at zero rate of shear, η_∞ (defined as $\eta_o(\sigma_2/\sigma_1)$) is the limiting viscosity at infinite rate of shear, and Γ is the shear rate. The viscous shear stress is described by $\tau = \eta\Gamma$.

Using the Oldroyd viscosity, Equation (2), the viscous shear stress can be illustrated graphically as in Figure 2a and 2b.

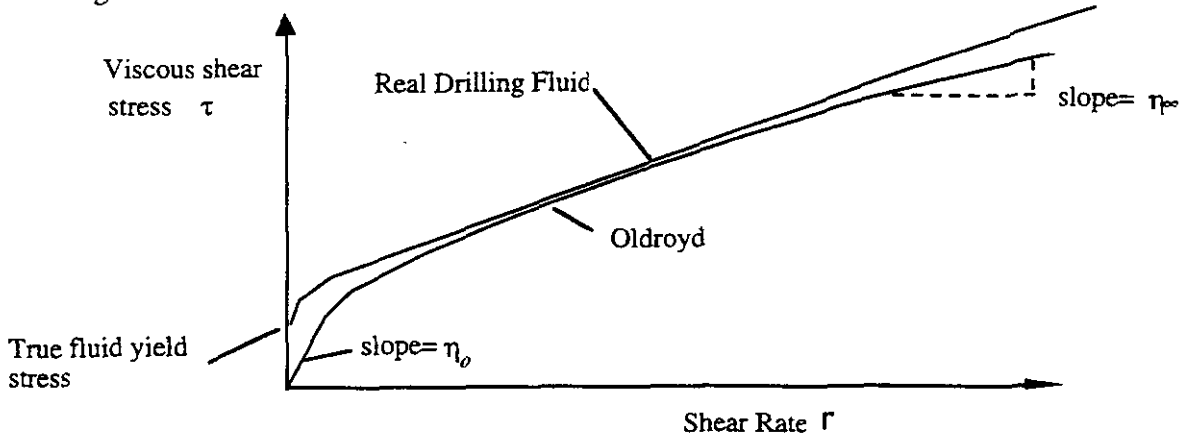

Figure 2a Oldroyd and real drilling fluid

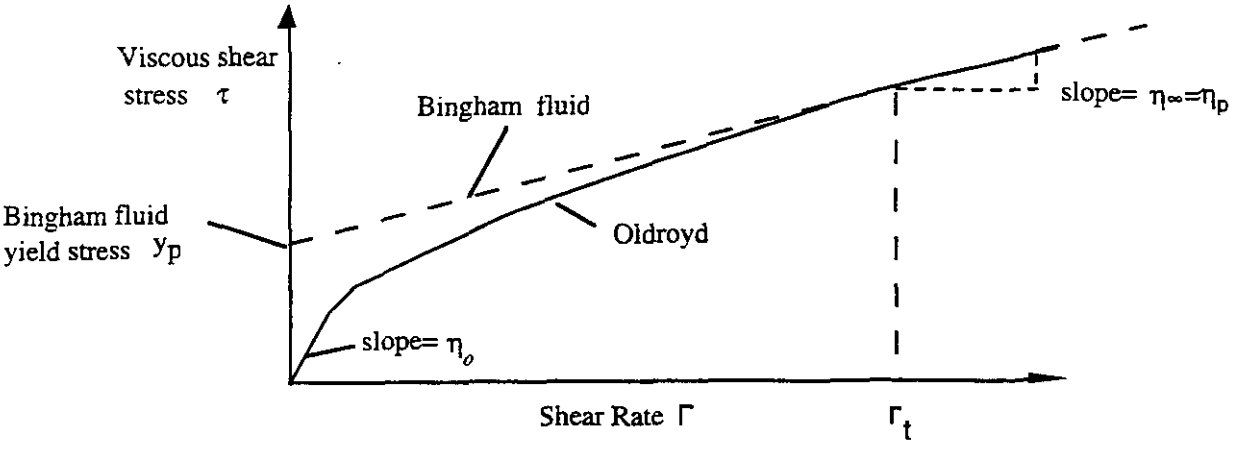

Figure 2b Oldroyd and Bingham fluid

This is a rate softening (pseudoplastic) model that has an initial slope of η_o and a limiting slope of η_∞ for large shear rates.

The Oldroyd model cannot account for drilling fluids that exhibit a yield stress. However, above a shear rate of zero, parameters can be chosen so that the model can be made to approximate the pseudoplastic rate response of many drilling fluids (see Figure 2).

Savins and Wallick (1966), expanding on the work of Coleman and Noll (1959) and Fredrickson (1960), showed that the solution for laminar helical flow of a non-Newtonian fluid in an annulus could be written in terms of three nonlinear integral equations.

$$F_1 = \int_{\alpha}^{1}\left(\frac{\rho^2-\lambda^2}{\rho}\right)\frac{d\rho}{\eta} = 0$$

$$F_2 = C\int_{\alpha}^{1}\frac{d\rho}{\rho^3\eta} - \Delta\Omega = 0 \qquad (3)$$

$$F_3 = \frac{4Q}{\pi R^3} + 4\left(\frac{RJ}{2}\right)\int_{\alpha}^{1}\left(\frac{\alpha^2-\rho^2}{\eta}\right)\left(\frac{\rho^2-\lambda^2}{\rho}\right)d\rho = 0$$

where α is the ratio of the collar radius over the cutting radius (R_i/R) (Figure 3), $\Delta\Omega$ is the drill string angular velocity, Q is the drilling fluid (mud) flow rate, r is the radial coordinate, and ρ is the non-dimensional radial coordinate representing the ratio r/R.
The unknown parameters λ^2, $RJ/2$, and C are related to the fluid shear stresses through the relations

$$\tau_{r\theta} = \frac{C}{\rho^2}$$

$$\tau_{rz} = \frac{RJ}{2}\left(\frac{\rho^2-\lambda^2}{\rho}\right) \qquad (4)$$

$$\tau^2 = \tau_{r\theta}^2 + \tau_{rz}^2$$

where r, θ, and z represent radial, tangential, and vertical coordinates associated with the cylindrical geometry of Figure 3.

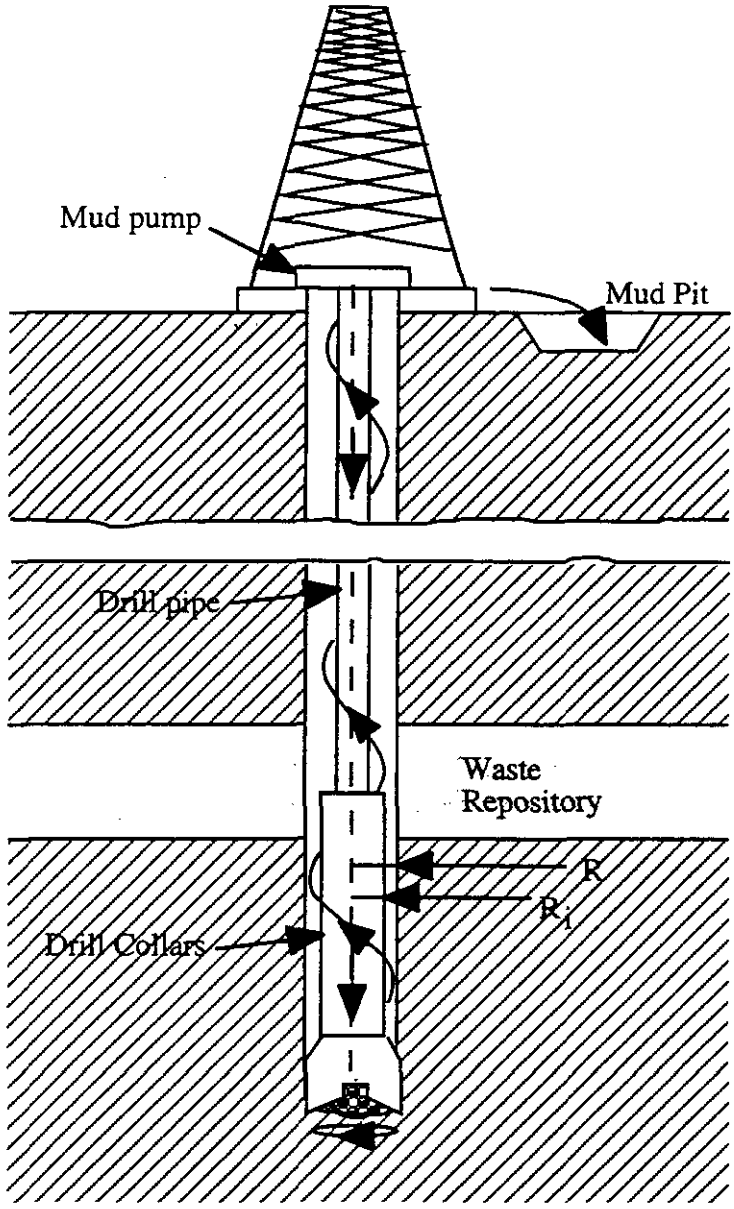

Figure 3. Detail of rotary drill string adjacent to repository.

The three nonlinear integral equations represented by (3) in general must be solved numerically. By expanding each of the integral equations into a Taylor series and retaining only the linear terms, a recursive solution procedure can be used (see Appendix AA)) to find the solution for the unknowns $\delta\lambda^2$, $\delta\left(\frac{RJ}{2}\right)$, and δC. The three linear equations are

$$\begin{aligned}
\frac{\partial F_1}{\partial \lambda^2}\delta\lambda^2 + \frac{\partial F_1}{\partial C}\delta C + \frac{\partial F_1}{\partial\left(\frac{RJ}{2}\right)}\delta\left(\frac{RJ}{2}\right) &= -F_1 \\
\frac{\partial F_2}{\partial \lambda^2}\delta\lambda^2 + \frac{\partial F_2}{\partial C}\delta C + \frac{\partial F_2}{\partial\left(\frac{RJ}{2}\right)}\delta\left(\frac{RJ}{2}\right) &= -F_2 \\
\frac{\partial F_3}{\partial \lambda^2}\delta\lambda^2 + \frac{\partial F_3}{\partial C}\delta C + \frac{\partial F_3}{\partial\left(\frac{RJ}{2}\right)}\delta\left(\frac{RJ}{2}\right) &= -F_3
\end{aligned} \qquad (5)$$

The solution procedure consists of assuming initial values for λ^2, $\left(\frac{RJ}{2}\right)$, and C and solving the three linear equations in (5) for the corrections $\delta\lambda^2$, $\delta\left(\frac{RJ}{2}\right)$, and δC. The unknowns λ^2, $\left(\frac{RJ}{2}\right)$, and C are then replaced by $\lambda^2 + \delta\lambda^2$, $\left(\frac{RJ}{2}\right) + \delta\left(\frac{RJ}{2}\right)$, and $C + \delta C$. This recursive solution procedure is repeated until $|\delta\lambda^2|$, $\left|\delta\left(\frac{RJ}{2}\right)\right|$, and $|\delta C|$ are all less than some specified limit.

The coefficients of the unknowns $\delta\lambda^2$, $\delta\left(\frac{RJ}{2}\right)$, and δC in equations (5) are determined by differentiating equations (3). These derivatives are:

$$\frac{\partial F_1}{\partial \lambda^2} = -\int_\alpha^1 \frac{1}{\eta\rho}\left[1+\frac{(\rho^2-\lambda^2)}{\eta}\frac{\partial \eta}{\partial \lambda^2}\right]d\rho$$

$$\frac{\partial F_1}{\partial C} = -\int_\alpha^1 \frac{1}{\eta\rho}\frac{(\rho^2-\lambda^2)}{\eta}\frac{\partial \eta}{\partial C}d\rho$$

$$\frac{\partial F_1}{\partial\left(\frac{RJ}{2}\right)} = -\int_\alpha^1 \frac{1}{\eta\rho}\frac{(\rho^2-\lambda^2)}{\eta}\frac{\partial \eta}{\partial\left(\frac{RJ}{2}\right)}d\rho$$

$$\frac{\partial F_2}{\partial \lambda^2} = -C\int_\alpha^1 \frac{1}{\eta^2\rho^3}\frac{\partial \eta}{\partial \lambda^2}d\rho$$

$$\frac{\partial F_2}{\partial C} = \int_\alpha^1 \frac{1}{\eta\rho^3}\left[1-\frac{C}{\eta}\frac{\partial \eta}{\partial C}\right]d\rho \qquad (6)$$

$$\frac{\partial F_2}{\partial\left(\frac{RJ}{2}\right)} = -C\int_\alpha^1 \frac{1}{\eta^2\rho^3}\frac{\partial \eta}{\partial\left(\frac{RJ}{2}\right)}d\rho$$

$$\frac{\partial F_3}{\partial \lambda^2} = -4\left(\frac{RJ}{2}\right)\int_\alpha^1 \frac{\alpha^2-\rho^2}{\eta\rho}\left[1+\frac{(\rho^2-\lambda^2)}{\eta}\frac{\partial \eta}{\partial \lambda^2}\right]d\rho$$

$$\frac{\partial F_3}{\partial C} = -4\left(\frac{RJ}{2}\right)\int_\alpha^1 \frac{(\alpha^2-\rho^2)}{\eta\rho}\frac{(\rho^2-\lambda^2)}{\eta}\frac{\partial \eta}{\partial C}d\rho$$

$$\frac{\partial F_3}{\partial\left(\frac{RJ}{2}\right)} = 4\int_\alpha^1 \frac{(\alpha^2-\rho^2)}{\eta\rho}(\rho^2-\lambda^2)d\rho - 4\left(\frac{RJ}{2}\right)\int_\alpha^1 \frac{(\alpha^2-\rho^2)}{\eta\rho}\frac{(\rho^2-\lambda^2)}{\eta}\frac{\partial \eta}{\partial\left(\frac{RJ}{2}\right)}d\rho$$

From equations (4) and using the relation $\tau = \eta\Gamma$ the viscosity can be related to the shear rate function $Y(\Gamma)$ by the equation

$$\eta^2 Y = 2\left[\left(\frac{RJ}{2}\right)^2\left(\frac{\rho^2-\lambda^2}{\rho}\right)^2+\frac{C^2}{\rho^4}\right] \qquad (7)$$

where

$$Y = 2\Gamma^2 \qquad (8)$$

For the Oldroyd viscosity function, equation (2), the unknown derivatives of the viscosity in equations (6) can be determined by using the chain rule of differentiation and equation (7).

$$\frac{\partial \eta}{\partial \lambda^2} = \frac{\partial(\eta^2 Y)}{\partial \lambda^2}\frac{\partial \eta}{\partial(\eta^2 Y)} = -4\left(\frac{RJ}{2}\right)^2\left(\frac{\rho^2-\lambda^2}{\rho^2}\right)\frac{\partial \eta}{\partial(\eta^2 Y)}$$

$$\frac{\partial \eta}{\partial C} = \frac{\partial(\eta^2 Y)}{\partial C}\frac{\partial \eta}{\partial(\eta^2 Y)} = \frac{4C}{\rho^4}\frac{\partial \eta}{\partial(\eta^2 Y)} \qquad (9)$$

$$\frac{\partial \eta}{\partial\left(\frac{RJ}{2}\right)} = \frac{\partial(\eta^2 Y)}{\partial\left(\frac{RJ}{2}\right)}\frac{\partial \eta}{\partial(\eta^2 Y)} = 4\left(\frac{RJ}{2}\right)\left(\frac{\rho^2-\lambda^2}{\rho}\right)^2\frac{\partial \eta}{\partial(\eta^2 Y)}$$

The derivative $\frac{\partial \eta}{\partial(\eta^2 Y)}$ can be determined by combining equations (2) and (8) and differentiating to obtain

$$\frac{\partial \eta}{\partial(\eta^2 Y)} = \frac{\left(\frac{\sigma_2}{2}\eta_o - \frac{\sigma_1}{2}\eta\right)^2}{\left(\frac{\sigma_2}{2}\eta_o - \frac{\sigma_1}{2}\eta\right)\left[\eta^2 + 2(\eta-\eta_o)\eta\right] + (\eta-\eta_o)\eta^2\frac{\sigma_1}{2}} \qquad (10)$$

A cubic equation for η in terms of the unknown parameters λ^2, $RJ/2$, and C can be written by combining equations (2), (7) and (8)

$$\eta^3 - \eta_o\eta^2 + \sigma_1\left[\left(\frac{RJ}{2}\right)^2\left(\frac{\rho^2-\lambda^2}{\rho}\right)^2 + \frac{C^2}{\rho^4}\right]\eta - \sigma_2\left[\left(\frac{RJ}{2}\right)^2\left(\frac{\rho^2-\lambda^2}{\rho}\right)^2 + \frac{C^2}{\rho^4}\right]\eta_o = 0 \qquad (11)$$

2.2.1.1 Solution Process for Laminar Flow

Laminar helical flow of an Oldroyd fluid in an annulus of a given size with a rotating inner core is based on the solution to the three integral equations (3) which have three unknown parameters λ^2, $RJ/2$, and C. A recursive process for computing the unknowns based on a Taylor series expansion (equation 5) requires the evaluation of the coefficients of the three linear equations. These coefficients (equations 6 combined with 9, 10, and 11) involve integrals across the radius of the annulus which must be integrated numerically. Simpson's 1/3 rule (Salvadori, et al 1962) is used to perform these integrations by dividing the annular radius into ten equal intervals. The initial solution obtained from the recursive process assumes no erosion has occurred and thus corresponds to an annulus with an outer radius equal to one half the borehole diameter. For the specific case of borehole erosion, once a solution to the unknowns (λ^2, $RJ/2$, and C) in the three integral equations in (3) is found, the shear stress in the fluid τ at the wall can be calculated by setting $\rho = 1$ in the equations in (4). By changing the outer radius of the hole and repeating the above process a new shear stress in the fluid at the wall can be calculated. By adjusting the outer radius appropriately the fluid shear stress can be forced to equal the repository effective shear resistance to erosion. That radius corresponds to the final eroded radius. The required outer hole radius is determined by iteration as shown in Figure 4. The derivatives required for the iteration $\left(\frac{d\tau}{dR}\right)$ are found numerically by determining the change in shear stress for a small assumed change in outer radius R.

Based upon the preceding equations a Fortran computer code was written to perform the necessary computations for a solution to the problem of laminar helical flow in an annulus. This code was partially verified by comparing its results against those published by Savins and Wallick (1966).

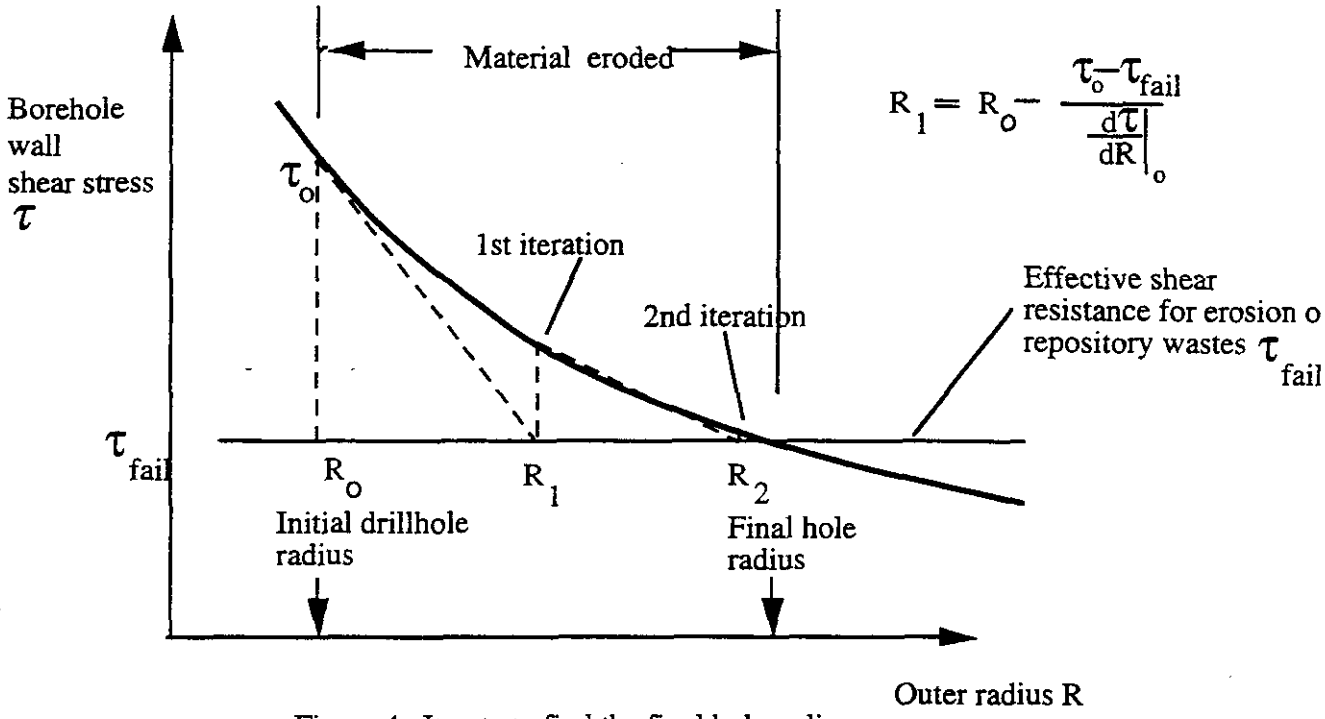

Figure 4. Iterate to find the final hole radius

The final eroded diameter is determined through an iterative process that equates the fluid shear stress adjacent to the waste to a measure of the erosion resistance of the waste. The erosion resistance is governed by the effective shear resistance to erosion, a parameter not directly related to the shear strength as normally determined for granular materials using conventional soil tests.

The effective shear resistance for erosion (τ_{fail}), equals the threshold value of fluid shear stress required to sustain general erosion at the borehole wall. Parthenaides and Passwell (1970), in discussing investigations on the erosion of seabed sediments and in channels, has noted that this effective soil shear resistance is not related to the soil shear strength as normally determined from conventional soil tests. The effective shear resistance for erosion based on seabed data, as determined by Parthenaides and Passwell (1970), is on the order of a few Pa and is thus smaller by several orders of magnitude than the macroscopic soil shear strength.

2.2.2 Turbulent Flow

For Newtonian fluids with Reynolds numbers greater than about 2100, flow in a circular pipe or annulus starts to become more or less random in character, which makes orderly mathematical

analysis of the flow difficult, if not impossible. With increasing Reynolds numbers, this random behavior increases until, at a Reynolds number of about 3000, the flow becomes fully turbulent. In fully turbulent flow, momentum effects dominate and the fluid viscosity is no longer important in characterizing pressure losses.

The Reynolds number (R_e) is defined as

$$R_e = \frac{\overline{\rho}\overline{V}D_e}{\overline{\eta}} \tag{12}$$

where D_e is the equivalent hydraulic diameter, $\overline{\rho}$ is the drilling fluid density, $\overline{V}$ is the average axial fluid velocity, and $\overline{\eta}$ is the average fluid viscosity.

For Newtonian fluids, the value to use for the viscosity is clear since the viscosity is constant for all rates of shear. Non-Newtonian fluids exhibit a changing viscosity with shear rate and present a special problem in calculating R_e. For fluids that exhibit a limiting viscosity at high rates of shear (such as the Bingham model and in our case the Oldroyd model), it has been suggested (Broc, 1982) that the limiting viscosity ($\overline{\eta} = \eta_\infty$) be used in calculating the Reynolds number.

The Reynolds number for an Oldroyd fluid in an annulus can then be written as (Broc, 1982)

$$R_e = \frac{0.8165 D_e \overline{V}\overline{\rho}}{\overline{\eta}} \tag{13}$$

where the equivalent hydraulic diameter is expressed as $D_e = 2(R - R_i)$ (see Figure 3).

The most important influence viscosity has on the calculation of pressure losses in fully turbulent flow of non-Newtonian fluids appears to be in the calculation of the Reynolds number. A far more important parameter is the surface roughness past which the fluid must flow. The Reynolds number, however, does have a role in determining the onset of turbulence. For Newtonian fluids this number is about 2100. For non-Newtonian, rate-thinning fluids, the critical value of R_e tends to be greater than 2100 but less than 2400 (Walker, 1976). For our purposes, a value of 2100 will be used to represent R_{e_c} (the critical Reynolds number) for the Oldroyd fluid model. Since turbulent flow is more effective in generating fluid shear stresses at the borehole wall, this assumption is conservative.

There is a transition region beyond R_{e_c} before the development of fully turbulent flow. In this regime the flow has the character of both laminar and turbulent flow. However, since pressure losses increase rapidly in turbulent flow and affect borehole shear stresses more severely, it will be assumed that beyond R_{e_c} the flow is fully turbulent.

Turbulent flow is very complex and, thus, to characterize the turbulent flow regime, the great bulk of analysis has concentrated on empirical procedures. For axial flow in an annulus, the pressure loss under turbulent conditions can be approximated by (Broc, 1982)

$$\Delta P = \frac{2fL\overline{\rho}\overline{V}^2}{(0.8165)D_e} \tag{14}$$

where f is the coefficient of pressure head loss (Fanning friction factor) and L is the borehole length.

If the shear stress due to the flowing fluid is assumed to be uniformly distributed on the inner and outer surfaces of the annulus, it can be easily shown using Equation (14) that the shear stress is related to the average fluid velocity through the relation

$$\tau = \frac{f\overline{\rho}\overline{V}^2}{2(0.8165)} \tag{15}$$

The Fanning friction factor is empirically related to the Reynolds number and relative roughness by the equation (Whittaker, 1985)

$$\frac{1}{\sqrt{f}} = -4\log_{10}\left[\frac{\varepsilon}{3.72D} + \frac{1.255}{R_e\sqrt{f}}\right] \tag{16}$$

where ε/D is the relative roughness. For circular pipes, D in this equation represents the inside diameter and ε is the absolute roughness or the average depth of pipe wall irregularities. In the absence of a similar equation for flow in an annulus, it is assumed that this equation also applies here, where D is the equivalent hydraulic diameter (D_e) as defined earlier and ε is the absolute roughness of the waste-borehole interface.

For laminar flow within the annulus both axial and rotational flow are modeled. Some of the available literature (Khader and Rao, 1974 ; Bilgen E., Boulos, R., and Akgungor A.C., 1973) indicates the importance of also accounting for drillstring rotation when the drilling mud flow within the annulus is turbulent. Consequently, to account for rotational flow in the turbulent regime, an axial flow velocity correction factor (rotation factor) is introduced into the above formulation that maintains eroded diameter compatibility across the laminar- turbulent flow transition. The rotation factor (F_r) is determined by increasing (or decreasing) the axial velocity $\overline{V}$ in equation 15 until the turbulent flow eroded diameter equals the laminar flow eroded diameter computed at the prescribed angular velocity at a Reynolds number of 2100. The rotation factor is defined as

$$F_r = \frac{\overline{V}_{2100}}{\overline{V}}$$

where $\overline{V}_{2100}$ is the axial velocity required for eroded diameters to be the same for turbulent and laminar flow. This rotation factor is then used to modify the axial turbulent flow velocity at all other turbulent flow Reynolds numbers. The rotation factor is not used when computing the Reynolds number. Equation 15 then can be rewritten

$$\tau = \frac{f\overline{\rho}\left(F_r\overline{V}\right)^2}{2(0.8165)} \tag{17}$$

2.2.2.1 Solution process for turbulent flow

Using a relative roughness and a calculated Reynolds number based on $\overline{V}$, a Fanning friction factor can be determined by iteratively solving Equation (16). The value of the shear stress acting on the borehole wall can then be determined from Equation (17). Using an iterative procedure similar to that for the laminar flow problem, the fluid shear stress can be forced to equal the repository shear resistance to erosion (τ_{fail}) to obtain the final eroded borehole radius (see Figure 4).

The equations governing cavings (and cuttings) based on laminar and turbulent flow form a portion of the Fortran computer code CUTTINGS_S (see figure 1). Using appropriately selected input based on the physical properties of the waste and other drilling parameters, this section of the code calculates the final eroded diameter of the borehole that passes through the waste. In the actual solution sequence employed in the fortran code the Reynolds number is calculated first to determine which solution regime (laminar or turbulent) should first be initiated. For Reynolds

numbers initially less than R_{ec} the code calculates the flow as laminar. Any increase in diameter of the borehole calculated during the laminar calculation will cause the Reynolds number to decrease ensuring that the calculation remains laminar. If the initial Reynolds number is greater than or equal to R_{ec} the turbulent formulation is used to calculate borehole erosion. When the turbulent calculation is complete, a check is again made to determine if the Reynolds number still exceeds R_{ec}. If it does not, the laminar calculation is performed starting with a "critical" borehole radius. The critical borehole radius corresponds to a Reynolds number of R_{ec} and is given by

$$R_{crit} = \frac{\bar{\rho} Q}{1286 \pi \eta_\infty} - R_i \tag{18}$$

2.3 Drilling parameters for cuttings and cavings

The drilling parameters chosen must reflect data typical of that valid near the WIPP repository. For drilling operations through salt in the Delaware basin , the drilling mud most likely to be used is a brine (Pace's letter on pages A-159 through A-164 of (Rechard et al., 1990)), with the density cut somewhat with an emulsified oil. The mud density and viscosity parameters required in the laminar and turbulent regime erosion calculations can be estimated based on the assumption of the use of such a brine-based drilling mud. For the 1992 PA the drilling mud properties used were (Sandia WIPP Project 1992, Table 4.4-1):

Parameter	Median	Range			Units	Distribution Type
Density	1211	1139	-	1378	kg/m^3	Constructed
Bingham Plastic Viscosity η_p	0.00917	0.005	-	0.03	Pa·s	Constructed
Bingham Yield Stress y_p	4	2.4	-	19.2	Pa	Constructed

The values for plastic viscosity and yield stress correspond to parameters for a Bingham plastic fluid (Darley and Grey 1988 , p188) from which the Oldroyd parameters are derived.

If in equation (2) it is assumed that $\eta_\infty = \eta_o \left(\frac{\sigma_2}{\sigma_1} \right) = \eta_p$ where η_p is the Bingham plastic viscosity, and if $\eta_o = 2\eta_\infty$ (a trend based on other drilling muds (Darley and Grey 1988 , p242)) the following relationship can be derived.

$$\sigma_2 = \frac{\eta_p \Gamma_t - y_p}{2\Gamma_t^2 y_p} \tag{19}$$

where Γ_t is the shear rate at which the Oldroyd model and Bingham model coincide (Figure 2b). This shear rate is chosen to be 1020 1/s which corresponds to a reading at 600 rpm on a direct reading viscometer (Darley and Grey 1988 , p214).

For drilling through salt, the drilling speeds can vary from 40 to 220 rpm (Austin, 1983 and Pace's letter on pages A-159 through A-164 of (Rechard et al., 1990)). The most probable speed is about 70 rpm (Pace's letter on pages A-159 through A-164 of (Rechard et al., 1990)).

Mud flow rates are usually selected to be from 30 to 50 gallons/minute per inch of drill bit diameter (Austin, 1983) and usually result in flow velocities in the annulus between the drill collars and the borehole wall at or near the critical flow state (laminar-turbulent transition) (Pace's letter on pages A-159 through A-164 of (Rechard et al., 1990)).

The drill bit diameter is related to the total planned depth of the hole to be drilled. For gas wells in the 4000- to 10,000-foot range, it is likely that the drill bit used that passes through a waste room would have a diameter of 10.5 to 17.5 inches. The most probable drill diameter is 12.25 inches. The collar diameter is assumed to be 8 inches, a value consistent with current drilling practice in the Delaware Basin (Marquis, 1995). For the 1992 PA these parameters are presented in table 4.2-1 (Sandia WIPP Project 1992)

Parameter	Median	Range			Units	Distribution Type
Drill bit diameter	0.355	0.267	-	0.444	m	Uniform
Drill string angular velocity	7.7	4.2	-	23	rad/s	Constructed
Drilling mud flowrate	0.09935	0.0745	-	0.124	$m^3/(s \cdot m)$	Uniform

For turbulent flow, the shear stress acting at the borehole at the repository is dependent on the absolute surface roughness. The value chosen for the calculations exceeds that of very rough concrete or riveted steel piping (Streeter, 1958).

The amount of material eroded from the borehole wall is dependent upon the magnitude of the fluid-generated shear stress acting on the wall and the effective shear resistance to erosion of the compacted, decomposed waste. In the absence of experimental data, the effective shear resistance to erosion of the repository material is assumed to be similar to that of a ocean bay mud (Parthenaides and Passwell, 1970), or a montmorillonite clay, (Sargunam et al., 1973). These values are on the order of a fraction to several Pa.

For the 1992 PA, the roughness and shear resistance parameters were given in table 3.4-1 (Sandia WIPP Project 1992).

Parameter	Median	Range			Units	Distribution Type
Absolute roughness	0.025	0.01	-	0.04	m	Uniform
Erosion shear resistance	1	0.05	-	10	Pa	Constructed

The lower bound to erosion resistance shown above is lower than that used in the 1992 PA and is based on the availability of additional data (Parthenaides and Passwell, 1970).

The hydrostatic pressure at the repository depth resulting from 1211 kg/m^3 drilling mud corresponds to 7.78 MPa. In the CUTTINGS_S code repository pressures below 8 MPa are assumed to cause surface releases from cuttings and cavings. Above 8 MPa releases are caused by spall (see figure 1).

2.4 Spallings

Spallings comprises that quantity of solid waste that reaches the ground surface as the result of the high pressure gas in the waste. If the repository gas pressure exceeds the hydrostatic pressure of the column of drilling fluid, solids releases can occur from blowout, stuck pipe or gas erosion. Contaminated brine can also be expelled during a blowout event, a process not considered in the CUTTINGS_S code. Brine releases to the surface resulting from blowout are computed using a separate code.

2.4.1 Blowout (Solids Removal)

Blowout is assumed to occur when repository gas pressures exceed 8 MPa (~hydrostatic) and when waste permeabilities exceed 10^{-16} m^2 (see figure 1). For permeabilities that are lower than 10^{-16} m^2 the gas flow into the borehole is assumed to be too low to cause well blowout (Berglund 1994).

Two alternative computational models are used to compute the solid waste released to the surface resulting from the sudden penetration of a pressurized WIPP panel. The models assume waste strength based on brine saturation and are self limiting ie. neither model relies on driller response. Of the two models described below, model 2 is more consistent with data obtained from experiment.

2.4.1.2 Solids Removal Caused by Blowout (Model 1)

A borehole penetration of a WIPP panel saturated by decomposition gases at pressures above hydrostatic and with a waste permeability greater than 10^{-16} m^2 is likely to initiate a blowout of the well. The initial flow of gas into the borehole will be restricted somewhat by the presence of drilling mud and a backpressure may develop that could be greater than hydrostatic. As the gas flows into the borehole and rises due to buoyancy, the backpressure will diminish as the weight of the mud column decreases. With a decreasing backpressure the gas flowrate into the borehole will increase. It will also increase as the result of the removal of waste material and the generation of a larger surface through which the gas can flow. Eventually the borehole will be cleared of drilling mud and the backpressure will drop to a value governed by the rate of flow of a compressible fluid in the drillstring annulus.

In the development of a bounding model for waste release due to a blowout it is important to note that the blowout process occurs over a finite time (minutes) and consequently it is not necessary to consider the high transient gas flow rates that occur from the assumption of instantaneous pressures drops. This is especially true for waste with high permeability where pressure profiles in the waste change rapidly. After these initial transients the gas flowrates out of an exposed waste surface become relatively constant for volumes comparable to a WIPP panel. It is this relative constancy of flow that allows for the development of the bounding model described below.

During blowout and after the decay of initial flow transients the gas velocity (V) at an exposed waste surface remains relatively constant for long periods of time. If the gas velocity is great enough and there is little cohesive strength between waste grains, the waste grains at this free

surface will be lofted into the flow of gas (entrained) and be carried into the borehole and to the ground surface. As the waste is removed and the exposed waste surface area increases, the resistance to flow up the borehole annulus increases causing a backpressure to develop in the evacuated volume. Consequently, the velocity of gas at this interface will decrease, eventually reaching a condition where waste is no longer entrained into the flowing gas at the waste surface. At this point an equilibrium condition will have been achieved and the volume associated with the dimensions of the exposed surface will be equal to a bounding waste release due to blowout.

The volume released is dependent on the shape of the void produced near the borehole. The shape is dependent on the waste properties and the character of the release process. A possible shape may be similar to the relatively flat ellipsoidal form shown in Figure 5.

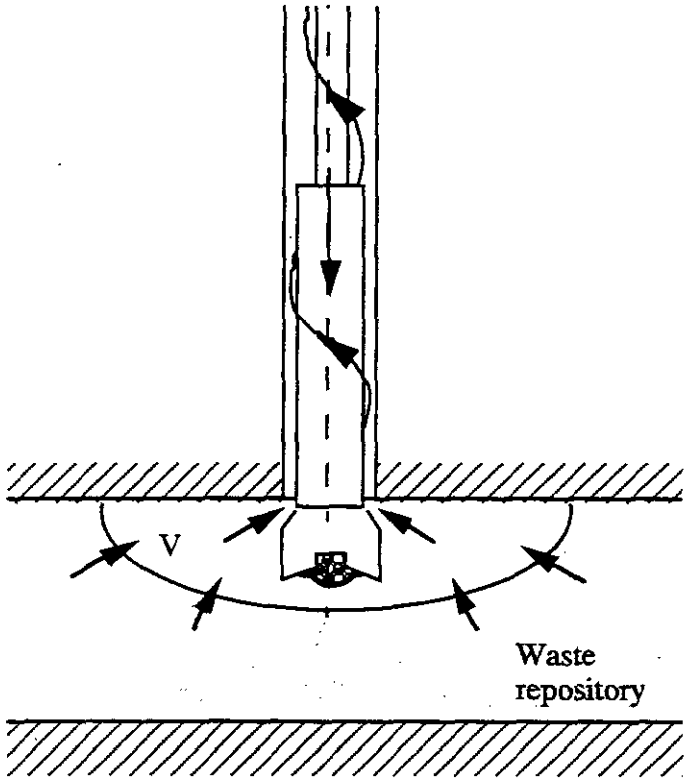

Figure 5 Potential Final Release Volume Configuration

A shape that provides a larger volume for the given exposed surface and one that is easy to calculate is the cylindrical volume shown in Figure 6.
The bounding blowout radius R_b (Figure 6) can then be written

$$R_b = \left[\left(\frac{D_o}{2}\right)^2 - \left(\frac{D_i}{2}\right)^2\right]\frac{M_f c}{2HV_e} \qquad (20)$$

where

D_o and D_i are the borehole and collar diameters
M_1 = the mach number for gas flow into the borehole entrance
c = the gas sound speed at the borehole entrance
H = the panel height at time of intrusion
V_e = the entrainment velocity

In this equilibrium condition the gas velocity V is equal to the entrainment velocity V_e and the solid waste volume released to the surface is

$$Volume = \pi R_b^2 H(1-\varphi) \tag{21}$$

where φ is the waste porosity at the time of intrusion. For the "actual" void shape (Figure 5), V_e is the gas velocity required to loft a waste particle vertically in a gravity field. This velocity is also used in the computational model where the void shape is assumed to be cylindrical.

As with cuttings (section 2.1), since the waste is assumed to be uniformly distributed throughout the disposal region, the actual computation for release requires only the area associated with R_b and the waste curie content per unit area. The panel height at the time of intrusion is related to the original height and waste porosity, and to the porosity at the time of intrusion.

$$H = \text{Initial height}\left(\frac{1-\text{intial porosity}}{1-\varphi}\right)$$

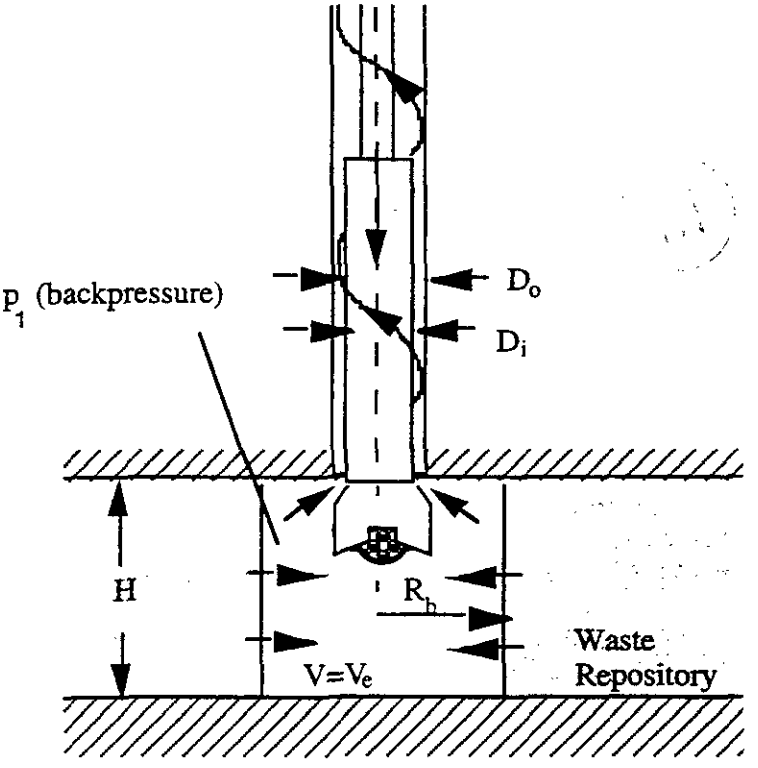

Figure 6 Idealized Cylindrical Final Volume Release Configuration

The borehole entrance mach number is computed based on flow in the borehole annulus and assumes that the borehole is free of drilling mud and undergoing full blowout. Compressible, isothermal flow in a channel (the borehole annulus) with friction is governed by the equation (Binder, 1958)

$$\frac{fl}{D} = \frac{1}{KM_1^2}\left[1-\frac{p_2^2}{p_1^2}\right] - 2\ln\frac{p_1}{p_2} \qquad (22)$$

where f=friction factor, D=pipe diameter, l =pipe length, K=ratio of specific heats of the gas, p_1 and p_2= inlet and outlet gas pressures, and M_1= inlet Mach number. The pipe diameter to use for our purposes is the effective hydraulic diameter computed from the annular area. Actually there are two annular areas that are considered for flow up the borehole; one area is adjacent to the drill collars and the other is adjacent to the drill pipe and consequently equation (22) has to be solved over these two regions. The pressure ratio is based on the exit pressure at the ground surface ($p_2 \geq$ atmospheric) and the borehole entrance pressure p_1 (backpressure).

The entrainment velocity V_e is the magnitude of the gas velocity at the exposed waste surface that will cause waste particles to be removed from the surface and transported in the gas to the borehole. For a horizontal waste surface this velocity is assumed to be the terminal velocity of the particle. The terminal velocity is the speed at which a particle will fall in a motionless gas of density ρ_g. For the present model, choosing this value to represent V_e is conservative since the terminal velocity is less than the surface normal gas velocity required to vertically support the particle if the surface is inclined.

The terminal velocity of a spherical particle can be found by equating the particle weight to the drag force acting on the particle when traveling at a velocity V_e. The relationship that results is (Cheremisinoff, 1984)

$$V_e^2 = \frac{4gd(\rho_s - \rho_g)}{3C_D\rho_g} \qquad (23)$$

where g= acceleration of gravity, d= particle diameter, ρ_s = particle density, ρ_g = gas density, and C_D is the coefficient of drag. The coefficient of drag for a sphere is an empirical function of the particle reynolds number R_{ed} (Fox et. al. 1973)

$$\text{where } R_{ed} = \frac{\rho_g V_e d}{\mu} \text{ and } \mu \text{ is the gas viscosity}$$

For $R_{ed} < 0.4$ $\quad C_D = \frac{24}{R_{ed}}$

For $0.4 < R_{ed} < 200000$ the data can be fit with the following function

$$C_D = 10^{(\bar{a}+\bar{b}x+\bar{c}x^2+\bar{d}x^3+\bar{e}x^4+\bar{f}x^5+\bar{g}x^6)} \qquad (24)$$

where

$$\bar{a} = 1.3918$$

$$\bar{b} = -0.907723$$

$$\bar{c} = 0.136371$$

$$\bar{d} = 0.0165093$$

$$\bar{e} = -0.0285484$$

$$\bar{f} = 0.00933281$$

$$\bar{g} = -0.000897166$$

and

$$x = log_{10} R_{ed}$$

For $R_{ed} > 200000$ $C_D = 0.2$

Equations (23) and (24) are solved simultaneously using an iterative process that converges to a value of V_e that satisfies both equations.

The velocity of gas flow (V) out of the cylindrical waste surface can be computed for various waste permeabilities and repository gas pressures using the equation

$$\frac{k}{2\mu}\nabla^2 p^2 = \varphi \frac{\partial p}{\partial t} \tag{25}$$

where k is the permeability, μ is the gas viscosity, φ is the waste porosity, $\nabla^2 = \frac{\partial^2}{\partial r^2} + \frac{1}{r}\frac{\partial}{\partial r}$, p is the gas pressure, and r is the radial coordinate. The rate is dependent on the pressure boundary condition (p_1) (Figure 6) assumed in the evacuated volume. The gas velocity in the waste at any radius r and time t is a function of the pressure gradient

$$v(r,t) = \frac{k}{\mu}\frac{\partial p(r,t)}{\partial r} \tag{26}$$

and the gas velocity at the free surface is $V = v(R_b,t)$ (27)

Solving equations (20), and (22-27) simultaneously and using stabilized flowrates out of the waste the bounding volumes of waste removed due to blowout can be obtained.

As observed earlier, the blowout process occurs over a finite time and the gas flowrate out of the free surface ($r=R_b$) tends to stabilize and remain constant for long periods of time. The time chosen to measure this "stable" flow condition has been chosen to be 700s after penetration. This is the minimum time necessary to replace the drilling mud in the annulus volume at the maximum expected drilling mud flowrate (50 gal/minute/inch of borehole diameter). This time is a measure of the minimum time necessary to generate full blowout.

The nonlinear partial differential equation for pressure in the waste (equation 25) can only be solved using numerical approximations (this is done in a code called GASFLOW) but the resulting solution is time consuming since it must be solved many times using different boundary conditions (p_1 and R_b). This process can be simplified by analytically solving the steady state form of equation 25 and by using a set of correction factors (calculated in GASFLOW) to obtain the free surface gas velocity at 700s. The steady state form of equation 25 is

$$\nabla^2 p^2 = 0 \tag{28}$$

The general solution to equation 28 is

$$p^2 = C_1 + C_2 \ln(r)$$

where

$$C_2 = \frac{p_1^2 - p_\infty^2}{\ln \frac{R_b}{R_\infty}} \tag{29}$$

$$C_1 = p_1^2 - C_2 \ln(R_b)$$

In these equations R_∞ is assumed to be the radius of an equivalent WIPP panel (~61m) and p_∞ is the far field gas pressure (ie. the initial pressure in the panel).
The steady state gas velocity at the free surface is

$$V(R_b) = \frac{k}{\mu}\frac{dp(R_b)}{dr} = \frac{k}{\mu}\frac{C_2}{2R_b(C_1 + C_2 \ln R_b)^{0.5}} \tag{30}$$

Equation 30 generally gives velocities lower than those that would be calculated from equation 26 using the GASFLOW code and setting the time to 700s. To be conservative in computing waste releases, the results from equation 30 should be at least as great as the velocities computed by GASFLOW at 700s. This is accomplished by multiplying the velocity calculated by equation 30 by a factor obtained from specific GASFLOW computations. For example, assuming the repository is pressurized with hydrogen gas (μ=9.3x10^{-6} Pa·s) the following velocity ratios

$$V_R = velocity\ ratio = \frac{Velocity\ from\ GASFLOW\ @\ 700s}{Steadystate\ velocity\ from\ equation\ 30} \tag{31}$$

are obtained for different radii R_b and waste permeabilities k.

let p_∞= 8x10^6 Pa, p_1= 1x10^6 Pa, φ_0=0.19, R_∞= 61m,
then

k (m^2)	velocity ratio V_R R_b=8m	velocity ratio V_R R_b=3m	velocity ratio V_R R_b=1m	velocity ratio V_R R_b=0.3m	velocity ratio V_R R_b=0.1 m
1x10^{-12}	0.558	0.734	0.836	0.897	0.92
1x10^{-13}	1.46	1.38	1.29	1.23	1.18
1x10^{-14}	2.75	2.19	1.78	1.53	1.12
1x10^{-15}	6.98	4.64	3.08	2.25	1.87
1x10^{-16}	20.5	12.23	6.68	3.90	2.79

equation 30 thus becomes

$$V(R_b) = \frac{k}{\mu} \frac{V_R C_2}{2R_b \left(C_1 + C_2 \ln R_b\right)^{0.5}} \tag{32}$$

A more complete set of tables for the velocity ratio data is shown in appendix AB. Data from these tables can be used to generate an equation for V_R as a function of the waste permeability. The fit corresponds to data values which produce the largest velocity ratio for a particular permeability. This process is conservative. See appendix AB. The resulting relationship for the velocity ratio is

$$V_R = -12593 - 5040\xi - 806.18\xi^2 - 64.455\xi^3 - 2.5771\xi^4 - 0.04125\xi^5 \tag{33}$$

where

$$\xi = log_{10} k$$

The terminal velocity described above (equations 23 and 24) is based on no cohesive strength between waste particles. Strength can be included in the model by changing the gravity term to that of an effective acceleration of gravity.

2.4.1.2.1 Effect of Strength on Solids Removal caused by Blowout

The model for solids removal during blowout is based on the lofting of particles from a horizontal surface of the waste as the result of the flow of escaping gas from the interior of the waste. Waste is lofted into the flowing gas if the velocity of the gas is equal to the terminal velocity of the waste particle. The equation for terminal velocity (equation 23) can again be written as

$$V_e^2 = \frac{4gd\left(\rho_s - \rho_g\right)}{3C_D \rho_g} \tag{34}$$

where g= acceleration of gravity, d= particle diameter, ρ_s = particle density, ρ_g = gas density, and C_D is the coefficient of drag.

The downward force resisting the drag force caused by the flowing gas is the weight of the particle. If there are additional forces acting to resist lofting such as tensile strength an effective gravity force can be computed and used to replace the gravity force in the terminal velocity equation.

Consider a material that has a tensile strength σ . This parting stress on the particle level can be written

$$\sigma = \frac{Parting \text{ force}}{\text{Particle projected area}} = \frac{mg_t}{\pi R^2} = \frac{\frac{4}{3}\pi R^3 \rho_s g_t}{\pi R^2} = \frac{4}{3}\rho_s g_t R \tag{35}$$

where m is the particle mass, R is the particle radius, ρ_s is the particle density and g_t is the effective acceleration of gravity necessary to generate a particle weight equal to the parting force.

Solving equation (35) for g_t obtains

$$g_t = \frac{3}{4}\frac{\sigma}{\rho_s R} \tag{36}$$

The effective acceleration of gravity that accounts for particle weight and strength can then be written

$$g_{eff} = (g + g_t) = g + \frac{3}{4}\frac{\sigma}{\rho_s R} \tag{37}$$

This effective acceleration of gravity can be used in the equation that computes the particle terminal velocity (equation 23) thus accounting for strength. A model for computing the parting stress based on waste saturation and particle size is presented in appendix AD. Additional contributions to strength, such as from cementation between particles, can also be included in the parting stress σ .

2.4.1.2.2 Solution Process for Solids Removal caused by Blowout (Model 1)

Utilizing Boyles Law which relates gas pressure to gas density it is possible to reduce equations 20, 22, 23, 24, and 32 to two simultaneous nonlinear equations in the unknowns R_b and the backpressure p_1. A solution process similar to that described in appendix AA was used to solve this system but it often failed to converge to the solution and was therefore considered unsuitable for use in a code where the input parameters were to vary over considerable ranges. To create a more robust solution to the system of equations, they are solved sequentially starting with equation 22.

As indicated earlier, flow in the borehole annulus is assumed to occur adjacent to both the drill collars and the drillpipe. Consequently, there are two annular areas that must be considered for flow up the borehole and equation (22) has to be solved over these two regions. The pressure ratio is based on the inlet and exit pressures for the two annuli with pressure compatibility maintained at the drillpipe / drill collar connection.

Utilizing conservation of mass, equation 22 can be divided into the two equations

$$\frac{fl_{coll}}{D_{coll}} = \frac{1}{KM_1^2}\left[1 - \frac{p_i^2}{p_1^2}\right] - 2\ln\frac{p_1}{p_i} \tag{38}$$

$$\frac{fl_{drill}}{D_{drill}} = \frac{1}{KM_1^2\left(\frac{p_1}{p_i}\right)^2\left(\frac{D_{coll}}{D_{drill}}\right)^4}\left[1 - \frac{p_{exit}^2}{p_i^2}\right] - 2\ln\frac{p_i}{p_{exit}} \tag{39}$$

where p_{exit}= exit pressure

l_{drill}= length of drillpipe

l_{coll}=collar length
D_{coll}=equivalent diameter of annulus opposite collars (based on annulus area)
D_{drill}=equivalent diameter of annulus opposite drillpipe (based on annulus area)
p_i=intermediate pressure

Eliminating M_1^2 from equations 38 and 39 results in a single nonlinear equation in the dependent variables p_i and p_{exit}.

$$F(p_i, p_{exit})=0 \tag{40}$$

A sequence of solutions to equation 40 for various backpressures p_1 are obtained by systematically scanning over possible values of p_i and p_{exit} and using the additional constraint (Binder, 1958 p 64) that either $\frac{dp}{dl}$ becomes unbounded at the pipe exit or $p_{exit}= p_{atm}$. Using this method results in a discrete set of p_1, M_1 pairs that satisfy equations 38 and 39.

Three equations remain to be satisfied; equations 20, 23 and 32.

For each p_1, the gas density can be determined from Boyles law and the terminal velocity V_e computed from equations 23 and 24 again using an iterative process. For the corresponding mach number in the p_1, M_1 pair it is now possible to compute R_b utilizing equation 20. The velocity V at the waste surface is then obtained from equation 32 using p_1 and R_b. For a valid solution the waste surface velocity V must equal the terminal velocity V_e. New p_1, M_1 pairs are selected sequentially until the V, V_e solutions approach equality and then linear interpolation is used for the final adjustment.

2.4.1.3 Solids Removal Caused by Blowout (Model 2)

Results from steady state flow experiments through granular material in a cylindrical geometry (Lary R. Lenke, et al. 1996) indicate that a porous pattern of channels is formed adjacent to the "borehole". This channeling process does not conform to conceptual model 1 as described above. As a consequence of these experiments a new conceptual model has been defined (model 2) which more closely corresponds to the physical processes that appear to be occurring. The new conceptual model is described below.

Conceptual model 2 is based on a number of assumptions. These are:

1. After intrusion by a drillbit, the pressure gradients associated with the flow of gas toward the borehole fracture the porous (waste) material sufficiently to permit the escaping gas to flow within the fractures rather than through the porous matrix (Figure 7). Consequently, the intrinsic permeability of the matrix no longer restricts gas flow and the gas pressure at the borehole entrance can be assumed to be the initial pore pressure.

2. The gas flow velocity up the borehole is governed by the isothermal flow of gas in a long tube of a given cross-sectional area, tube roughness, and gas pressure at the borehole entrance. (For sufficiently high borehole entrance pressures the flow velocity tends to choke or become self limiting.)

3. The mass flowrate of gas in the fractures at any radial cross-section away from the borehole is equal to the mass flowrate up the borehole.

4. Radial gas flow within the fractures of the waste matrix erode and widen the fractures. Erosion is assumed to occur if the fracture gas velocity exceeds a velocity v_e. (The higher gas velocities in fractures near the borehole create wider channels near the borehole.)

5. The fracture erosion velocity v_e is related to the terminal velocity of a waste particle at the fracture surface and to the cohesive strength afforded by moisture and cementation in the matrix. Experiments will determine the effectiveness of cohesive strength and gravity on erosion and will provide experimentally determined effectiveness factors F_{se} , F_{ge} , and F_{ce} which are related to these factors.

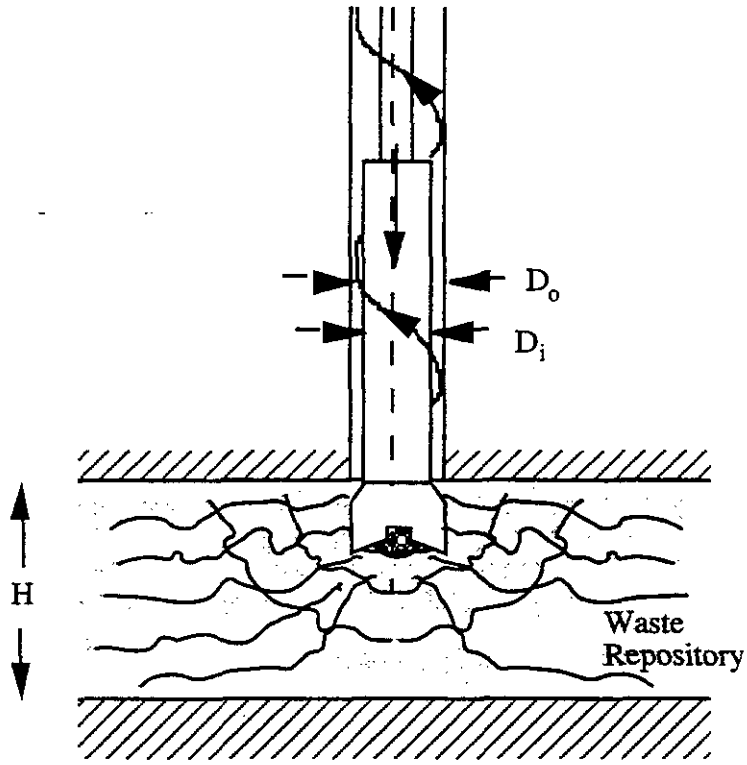

Figure 7 Fractured Waste Matrix after Penetration

2.4.1.3.1 Computation of Release Volume (Model 2)

Since the gas pressure is assumed to be constant throughout the fractured, porous matrix, conservation of mass flow requires (Figure 8)

$$2\pi rVH = A_{borehole}V_{borehole}$$

or

$$V = \frac{A_{borehole}V_{borehole}}{2\pi rH} \qquad (41)$$

where V is the average gas velocity within the matrix at a radius r from the borehole and H is the height of a repository room at the time of intrusion. The borehole annulus area is denoted as $A_{borehole}$ and the average gas velocity up the borehole annulus is denoted $V_{borehole}$.

The local gas velocity within the fractures (Figure 8) can be written as $v = \frac{V}{\varphi_f}$ where φ_f is the fracture porosity. Thus the fracture porosity associated the erosion fracture velocity v_e is

$$\varphi_{fe} = \frac{V}{v_e} = \frac{A_{borehole} V_{borehole}}{2\pi r H v_e} \tag{42}$$

The solid volume eroded from the fractures is

$$V_{ol} = 2\pi H(1-\phi)\int_0^{r_o} \varphi_{fe} r dr = \frac{A_{borehole} V_{borehole}}{v_e}(1-\phi)\int_0^{r_o} dr \tag{43}$$

or

$$V_{ol} = \frac{A_{borehole} V_{borehole} r_o}{v_e}(1-\phi) \tag{44}$$

where ϕ is the matrix porosity at the time of intrusion

Equation (44) indicates that the solid volume of material removed (spalled) due to a borehole penetration is a function of the flowrate up the borehole, the physical extend of a repository room, the waste porosity, and a velocity above which erosion occurs in waste fractures. The gas velocity up the borehole is a known function of the gas pressure at the borehole entrance.

2.4.1.3.2 Erosion Velocity (within fractures)

The fracture erosion velocity v_e is the average threshold gas velocity in a fracture required to "erode" the fracture walls. It is assumed to be related to the terminal velocity of a waste particle and to the cohesive strength between particles caused by pore water and cementation.

Equations 23 and 37 relate the gas velocity required to loft a waste particle to the weight of the particle and to the tensile strength required to separate two particles that are bonded by pore water and cementation. The resulting equation

$v_e^2 = \frac{4 g_{eff} d(\rho_s - \rho_g)}{3 C_D \rho_g}$ depends on an effective gravity term

$$g_{eff} = (g + g_t) = g + \frac{3}{4}\frac{\sigma}{\rho_s R} = g + \frac{3}{4}\frac{\sigma_p}{\rho_s R} + \frac{3}{4}\frac{\sigma_c}{\rho_s R}$$ where the parting stress (equation 37) is assumed to have contributions resulting from pore water σ_p and intergranular cementation σ_c. For the channeling model, since particle erosion is occurring in the channels

rather than lofting, correction factors are applied to the parting stresses and acceleration of gravity. Thus the effective gravity term becomes

$$g_{eff} = gF_{ge} + \frac{3}{4}\frac{\sigma_p}{\rho_s R}F_{se} + \frac{3}{4}\frac{\sigma_c}{\rho_s R}F_{ce} \qquad (45)$$

where F_{ge} is the gravity effectiveness factor and F_{se} and F_{ce} are the stress effectiveness factors. These constants are determined by experiment. Since the fracture erosion velocity v_e is dependent upon a coefficient of drag C_D which is in turn a function of v_e (see equation 24) an iterative solution process is used to converge to a solution for v_e.

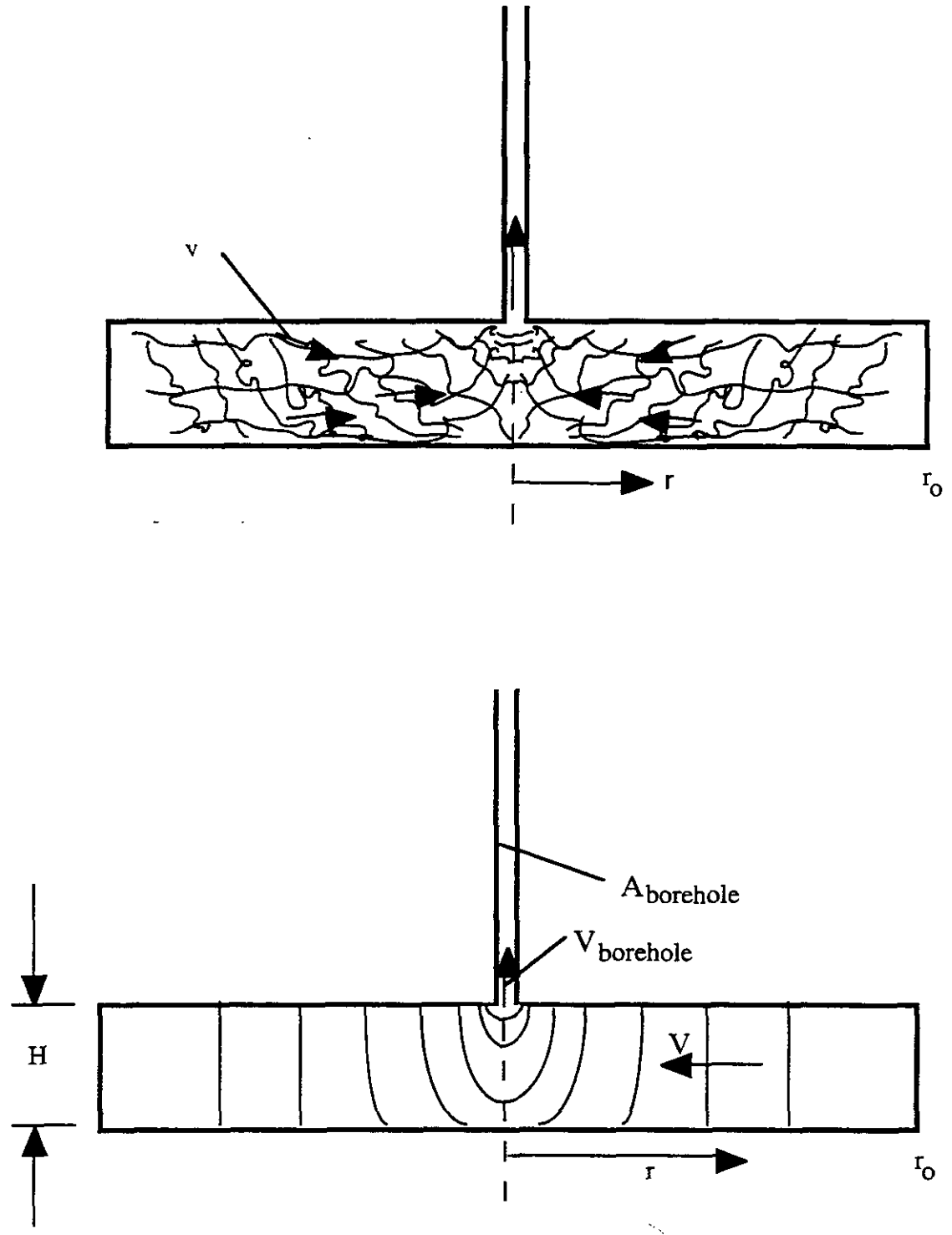

Figure 8 Flow Model

2.4.1.3.3 Solution Process for Solids Removal caused by Blowout (Model 2)

The solution to equation 44 requires 5 quantities. The value r_o is chosen as the equivalent radius of a repository room based on area. For a WIPP room r_o~ 17 m. The borehole area $A_{borehole}$ is detemined by the annulus area or (Figure 7)

$$A_{borehole} = \frac{\pi}{4}\left(D_o^2 - D_i^2\right)$$

To determine $V_{borehole}$ requires the solution of equation 22. As indicated earlier, flow in the borehole annulus is assumed to occur adjacent to both the drill collars and the drillpipe. Consequently, there are two annular areas that must be considered for flow up the borehole and equation (22) has to be solved over these two regions. The pressure ratio is based on the inlet and exit pressures for the two annuli with pressure compatibility maintained at the drillpipe / drill collar connection.

Utilizing conservation of mass, equation 22 can be divided into the two equations

$$\frac{fl_{coll}}{D_{coll}} = \frac{1}{KM_1^2}\left[1-\frac{p_i^2}{p_1^2}\right] - 2\ln\frac{p_1}{p_i} \qquad (46)$$

$$\frac{fl_{drill}}{D_{drill}} = \frac{1}{KM_1^2\left(\frac{p_1}{p_i}\right)^2\left(\frac{D_{coll}}{D_{drill}}\right)^4}\left[1-\frac{p_{exit}^2}{p_i^2}\right] - 2\ln\frac{p_i}{p_{exit}} \qquad (47)$$

where p_{exit}= exit pressure

l_{drill}= length of drillpipe
l_{coll}=collar length
D_{coll}=equivalent diameter for collar annulus (based on annulus area)
D_{drill}=equivalent diameter for drillpipe annulus (based on annulus area)
p_i=intermediate pressure
M_1=inlet Mach number

In addition to equations 46 and 47 the flow requires the additional constraint (Binder, 1958 p 64) that either $\frac{dp}{dl}$ becomes unbounded at the pipe exit or $p_{exit} = p_{atm}$. A recursive process based on Taylor series expansions (appendix AA) is used to obtain the solution to the three governing equations. Seed values used as initial guesses to the solution are obtained by systematically scanning over possible values of p_i and p_{exit} for a fixed backpressure (p_1= waste gas pore pressure).

The borehole velocity is related to the inlet Mach number by the relation

$$V_{borehole} = CM_1$$

where $C = (KRT)^{\frac{1}{2}}$ is the local sound speed, T is the absolute temperature and K and R are gas constants. For hydrogen gas K =1.41 and R = 4116. $\frac{Nm}{kg.s}$ (Obert, 1948, p541)

2.4.1.3.4 Determination of the factors F_{ge} and F_{se}

The gravity effectiveness factor F_{ge} and the stress effectiveness factors F_{se} and F_{ce} are required in equation (45) to compute an effective gravity term for use in model 2 (Section 2.4.1.3.1). Laboratory scale blowout experiments (SNL Contract AL 7022) have been performed which produce data on the volume of material ejected under various conditions of borehole diameter, gas pressure, waste particle size, etc. For arbitrarily selected values of the parameters F_{ge} , F_{se} and F_{ce} various degrees of fit to the data can be achieved. This process is conducted within the CUTTINGS_S code prior to performing any predictions of full scale response. In the present analysis a best fit is achieved when the sum of the squares of the differences in computed volumes and experimental volumes is a minimum for all data points.

Defining the error as E

$$E = \sum_{1}^{n}\left[V_{ei} - V_{mi}\left(F_{se}, F_{ge}, F_{ce}\right)\right]^2 \qquad (48)$$

where V_{ei} is the volume of waste simulant ejected in experiment i

$V_{mi}\left(F_{se}, F_{ge}, F_{ce}\right)$ is the computed volume of waste simulant ejected (calculated by CUTTINGS_S computer code)

n is the number of experiments

A best fit is achieved when F_{ge}, F_{se}, and F_{ce} are chosen such that E is a minimum.

For the set of n data points the computations defined by equation (48) are made within a module of the CUTTINGS_S computer code by scanning over a range of possible values of F_{ge}, F_{se}, and F_{ce}.

2.4.2 Stuck Pipe

If the waste has a low permeability when penetrated by a drillbit, the gas flow into the drilling mud may cause waste failure adjacent to the borehole (Berglund, 1993) and jam the drillbit preventing further drilling. Prior to becoming completely stuck the driller will notice an increase in torque on the drillstring and a decrease in the rotational speed. When sticking occurs the driller will usually initiate a cleanout procedure wherein the drill bit is raised and lowered repeatedly into the sticking formation to clear the obstruction. This process can be continued for as much as 12-24 hours if it is shown to be effective. After this time the problem must be solved by weighting up the mud, spot sealing with cement or setting casing (Short,1982).

During the cleanout procedure waste will be transported to the surface with each thrust of the drillbit into the obstruction. The quantity of waste removed is related to the maximum carrying capacity of the drilling mud and can be estimated based on the observation that for drill cutting loadings above 5% in the drilling mud (Darley & Gray, 1988, p259) tight hole conditions or stuck drillpipe may occur when circulation is stopped for any reason. Thus the maximum solid waste removal rate would consist of 5% of the drilling mud flowrate. The total quantity of solid waste transported to the surface can thus be computed as the waste removal rate multiplied by the cleanout time. The range of releases possible is based on variations in drillbit diameter (10.5 to 17.5 inches), duration of the cleanout procedure (12 to 24 hours) and the drilling mud flowrate (30 to 50 gallons/minute/inch of drill diameter). The releases are based on

$$V_S = 0.05 Q D_o T \qquad (49)$$

where

V_S= Solid waste volume brought to ground surface
Q=Drilling mud flow rate/drillbit diameter
T=Cleanout duration
D_o= Drill bit diameter

and varies between 43 to 238 m^3 of solid waste.

The lower limit of repository gas pressure at which sticking would occur (10MPa) is based on a drillstring power of 800hp and a coefficient of friction between the waste and drillcollars of 0.3. For these conditions the drill string angular velocity would decrease by more than 50% from the normal operating range alerting the driller to sticking conditions.

2.4.3 Gas Erosion

This again occurs when the waste has a low permeability and the gas flow to the borehole is very low and either is not detected by the driller or is allowed to trickle slowly along the drillstring and be released at the surface. The waste fails adjacent to the borehole perhaps causing some pipe sticking but the driller is able to continue and does not detect the unusual nature of the drill cuttings being brought to the surface. The flow of gas from the waste to the borehole generates a stress state in the waste adjacent to the borehole that depending on waste strength and the magnitude of the pressure gradient impresses the failed waste against the drillstring causing a continuous process of gas assisted erosion. As waste erodes more waste moves towards the drillstring in response to the gas pressure gradient and the process continues until sufficient gas has been released from the panel to preclude waste failure or until casing is set. Because the driller is either not aware of, or ignores the nature of the drill cuttings being removed in this case, the final volume of waste removed can be substantial.

For compacted waste with little or no strength waste failure will generally occur for all repository gas pressures that exceed the hydrostatic stress of the drilling mud. The failed waste is then transported to the accessible environment in the drilling mud. As with the sticking mode described above, the volume of waste removed can be computed based on the observation that above drill cutting loadings above 5% in the drilling mud (Darley & Gray, 1988, p259) tight hole conditions or stuck drillpipe may occur when circulation is stopped for any reason. Thus under these conditions the driller is not likely to remove waste to the surface at a rate faster than continuous drilling at the 5 percent limit.

The 5 percent cuttings loading will consist of both cuttings (from the hole bottom) and gas spallings. For a fixed mud flowrate the cuttings percentage will vary with the penetration rate. The penetration rate varies between 50 - 100 ft/hr. For high penetration rates the cuttings

percentage will be high leaving only a small amount for spallings to add up to the assumed 5 percent limit. For low penetration rates the cuttings percentage will be small and the spallings percentage correspondingly greater. The quantity of waste removed to the surface will be equal to (spall percentage) X (mud flowrate) X (drilling time). The drilling time is governed by the time required to drill from the elevation of the repository to the elevation at which casing is set which is below the Castile formation at 4500 ft.

The solid volume of waste brought to the surface can by readily computed based on available drilling parameters utilizing the following equation.

$$V_S=[0.05QD_o-\pi(D_o^2/4.)R_p]\Delta/R_p \qquad (50)$$

where

V_S= Solid waste volume brought to ground surface
Q=Drilling mud flow rate/drillbit diameter
D_o=Drill bit diameter
R_p=Penetration rate
Δ=Differential Drilling Depth (distance from repository depth to depth where casing is set)

Based on a differential drilling depth of 2350 ft, and placing the remaining variables at their extreme values the range of volumes of solid waste released to the surface ranges from 44 to 356 m^3.

3.0 Radionuclide Chains and Decay

The radionuclide inventory contained in the waste decays with time and follows several decay pathways or chains until stable elements are attained. The number of atoms of each radioactive waste constituent thus varies with time and the activity of waste brought to the surface as the result of human intrusion must account for the initial radionuclide inventory, the decay pathways, the mass of waste released, and the time of intrusion.

The radioactive decay of a chain of radionucides is governed by the Bateman equations and is described in Kaplan, 1962.

Consider a chain of n radionuclides where N_1, N_2, N_3, N_d .....N_n represent the number of atoms of each of the radionuclides in the repository and where N_n is stable. The differential equations that govern the decay and growth are

$$\frac{dN_1}{dt} = -\lambda_1 N_1$$

$$\frac{dN_2}{dt} = \lambda_1 N_1 - \lambda_2 N_2$$

$$\frac{dN_3}{dt} = \lambda_2 N_2 - \lambda_3 N_3 \qquad (51)$$

.....

.....

$$\frac{dN_n}{dt} = \lambda_{n-1} N_{n-1}$$

It will be assumed that the initial number of atoms of radionuclide 1 in the repository is N_1^0 and the initial number of atoms of the daughter atoms are N_2^0, N_3^0, N_4^0 .....N_n^0. The disintegration constants are λ_1, λ_2, λ_3, λ_4 .....λ_{n-1} . The half lives of the radionuclides are related to the disintegration constants through the relation, $t_{\frac{1}{2}}$ =half life $= \frac{ln\,2}{\lambda}$. Solving the differential equations (7) sequentially

obtains $$N_n = \sum_{j=1}^{n} N_j^0 \prod_{i=j}^{n-1} \lambda_i \sum_{i=j}^{n} \left(\prod_{l=j+1}^{n} \frac{1}{\lambda_l - \lambda_i} \right) e^{-\lambda_i t} \qquad (52)$$

where t is the decay time at the time of intrusion.

Additional details of this derivation are shown in Appendix AC.
The activity (in curies) of each radionucide is related to the number of atoms through the relation (Sandia WIPP Project. 1992, Table 15) $A_i = \frac{1.128x10^{16} N_i}{t_{\frac{1}{2}} M_i}$ where M_i is the gram molecular weight of the ith radionuclide. The activity in curies of the ith radionuclide released to the surface resulting from a human intrusion (a_i) is determined by mutiplying the repository activity A_i by the percent of waste removed or

$$a_i = A_i \left(\frac{Volume\ Released}{Repository\ Volume} \right) = A_i \left(\frac{Projected\ Area\ Removed}{Repository\ Area} \right)$$

Appendix AA

Recursive process for solving a system of non-linear equations (Salvadori, et al 1962)

Given a system of non-linear equations (in our case 3 equations) in the unknowns x,y,z of the form

$$F_1(x,y,z) = 0$$
$$F_2(x,y,z) = 0 \qquad (A1)$$
$$F_3(x,y,z) = 0$$

A recursive solution procedure can be developed by expanding the equations in Taylor series about an initial guess (x_o, y_o, z_o) for the solution.

$$\begin{aligned}
F_1(x,y,z) &= F_1(x_o,y_o,z_o)+\frac{\partial F_1(x_o,y_o,z_o)}{\partial x}(x-x_o)+\frac{\partial F_1(x_o,y_o,z_o)}{\partial y}(y-y_o)+\frac{\partial F_1(x_o,y_o,z_o)}{\partial z}(z-z_o)+\ldots=0\\
F_2(x,y,z) &= F_2(x_o,y_o,z_o)+\frac{\partial F_2(x_o,y_o,z_o)}{\partial x}(x-x_o)+\frac{\partial F_2(x_o,y_o,z_o)}{\partial y}(y-y_o)+\frac{\partial F_2(x_o,y_o,z_o)}{\partial z}(z-z_o)+\ldots=0\\
F_3(x,y,z) &= F_3(x_o,y_o,z_o)+\frac{\partial F_3(x_o,y_o,z_o)}{\partial x}(x-x_o)+\frac{\partial F_3(x_o,y_o,z_o)}{\partial y}(y-y_o)+\frac{\partial F_3(x_o,y_o,z_o)}{\partial z}(z-z_o)+\ldots=0
\end{aligned} \tag{A2}$$

Retaining only the linear terms of the Taylor series and defining

$$\begin{aligned}
\delta x &= x - x_o\\
\delta y &= y - y_o\\
\delta z &= z - z_o
\end{aligned} \tag{A3}$$

three linear simultaneous equations result

$$\begin{aligned}
\frac{\partial F_1(x_o,y_o,z_o)}{\partial x}\delta x+\frac{\partial F_1(x_o,y_o,z_o)}{\partial y}\delta y+\frac{\partial F_1(x_o,y_o,z_o)}{\partial z}\delta z+F_1(x_o,y_o,z_o)=0\\
\frac{\partial F_2(x_o,y_o,z_o)}{\partial x}\delta x+\frac{\partial F_2(x_o,y_o,z_o)}{\partial y}\delta y+\frac{\partial F_2(x_o,y_o,z_o)}{\partial z}\delta z+F_2(x_o,y_o,z_o)=0\\
\frac{\partial F_3(x_o,y_o,z_o)}{\partial x}\delta x+\frac{\partial F_3(x_o,y_o,z_o)}{\partial y}\delta y+\frac{\partial F_3(x_o,y_o,z_o)}{\partial z}\delta z+F_3(x_o,y_o,z_o)=0
\end{aligned} \tag{A4}$$

Based on an initial trial solution (x_o, y_o, z_o) sufficiently "close" to the actual solution, the three linear equations (A4) can be solved for the increments δx, δy, and δz and new values for x, y, and z can be determined from equations (A3). This process can be repeated until $|\delta x|$, $|\delta y|$, and $|\delta z|$ are less than a specified limit.

Appendix AB
Velocity ratio factors

Calculation of blowout releases using the model of section 2.4.1 requires the value of the gas velocity escaping from a cylindrical waste surface 700s after the drill bit has breached the repository. Since the solution process for the final blowout radius is iterative, the required gas velocity has to be determined many times using a large number of blowout radii. Although this velocity can be computed using the finite difference code GASFLOW, the code is slow and the total computation time necessary would be prohibitive. Therefore rather than using the results of the GASFLOW directly in the computational model a corrected steady state model is used which can be solved quickly in closed form. To calculate conservative blowout releases the steady state model should generate releases at least as great as those that would be predicted using the computationally intensive GASFLOW code. The correction factors required for this are

determined by running both GASFLOW and the steady state model over a range of boundary and initial conditions and by computing the velocity ratios given by

$$V_R = velocity\ ratio = \frac{Velocity\ from\ GASFLOW\ @\ 700s}{Steadystate\ velocity\ from\ equation\ 28}$$

Tabulated values for V_R are given below for a number of cases which cover a wide variable range. By choosing the largest V_R value for a given permeability (indicated in each table) a fit to the data using permeability as the independent variable can be made.

$k=10^{-16}m^2$	p_∞=8 MPa p_1=1Mpa			p_∞=15 MPa p_1=1Mpa		
R_b (m)	φ=0.09	φ=0.19	φ=0.29	φ=0.09	φ=0.19	φ=0.29
0.1	2.41	2.79	3.04	2.17	2.47	2.68
0.3	3.20	3.90	4.40	2.76	3.30	3.69
1.0	5.09	6.68	7.87	4.13	5.31	6.2
3.0	8.82	12.23	14.8	6.81	9.32	11.2
8.0	14.4	20.5	25.1	10.8	15.3	18.7
13.0	17.4	24.9	30.6	12.9	18.5	22.7
20.0	19.0	27.4	33.7	14.1	20.3	24.9

$k=10^{-15}m^2$	p_∞=8 MPa p_1=1Mpa			p_∞=15 MPa p_1=1Mpa		
R_b (m)	φ=0.09	φ=0.19	φ=0.29	φ=0.09	φ=0.19	φ=0.29
0.1	1.69	1.87	1.99	1.56	1.71	1.82
0.3	1.96	2.25	2.45	1.76	2.00	2.16
1.0	2.52	3.08	3.48	2.17	2.6	2.91
3.0	3.55	4.64	5.46	2.89	3.71	4.31
8.0	5.07	6.98	8.42	3.94	5.35	6.41
13.0	5.86	8.21	9.99	4.47	6.21	7.51
20.0	6.25	8.85	10.8	4.71	6.62	8.07

$k=10^{-14}m^2$	p_∞=8 MPa p_1=1Mpa			p_∞=15 MPa p_1=1Mpa		
R_b (m)	φ=0.09	φ=0.19	φ=0.29	φ=0.09	φ=0.19	φ=0.29
0.1	1.29	1.12	1.46	1.21	1.3	1.36
0.3	1.38	1.53	1.63	1.28	1.40	1.49
1.0	1.54	1.78	1.94	1.40	1.58	1.70
3.0	1.80	2.19	2.47	1.56	1.85	2.07
8.0	2.13	2.75	3.22	1.77	2.22	2.57
13.0	2.28	3.03	3.60	1.86	2.39	2.80
20.0	2.3	3.12	3.74	1.87	2.42	2.87

$k=10^{-13}m^2$	p_∞=8 MPa p_1=1Mpa			p_∞=15 MPa p_1=1Mpa		
R_b (m)	$\varphi=0.09$	$\varphi=0.19$	$\varphi=0.29$	$\varphi=0.09$	$\varphi=0.19$	$\varphi=0.29$
0.1	1.17	1.18	1.19	1.11	1.18	1.19
0.3	1.20	1.23	1.24	1.12	1.20	1.22
1.0	1.22	1.29	1.32	1.11	1.24	1.28
3.0	1.25	1.38	1.44	1.09	1.28	1.35
8.0	1.24	1.46	1.58	1.00	1.28	1.41
13.0	1.18	1.48	1.63	0.881	1.23	1.40
20.0	1.03	1.40	1.60	0.677	1.09	1.31

$k=10^{-12}m^2$	p_∞=8 MPa p_1=1Mpa			p_∞=15 MPa p_1=1Mpa		
R_b (m)	$\varphi=0.09$	$\varphi=0.19$	$\varphi=0.29$	$\varphi=0.09$	$\varphi=0.19$	$\varphi=0.29$
0.1	0.692	0.929	1.03	0.460	0.735	0.872
0.3	0.631	0.897	1.01	0.394	0.678	0.831
1.0	0.537	0.836	0.980	0.305	0.587	0.758
3.0	0.414	0.734	0.911	0.208	0.464	0.645
8.0	0.257	0.558	0.762	0.111	0.301	0.467
13.0	0.164	0.416	0.617	0.0646	0.200	0.337
20.0	0.0816	0.253	0.419	0.0292	0.106	0.198

The values of V_R and permeability k are thus

V_R	k
33.7	10^{-16}
10.8	10^{-15}
3.74	10^{-14}
1.63	10^{-13}
1.03	10^{-12}

These can be fit with the function

$$V_R = -12593 - 5040\xi - 806.18\xi^2 - 64.455\xi^3 - 2.5771\xi^4 - 0.04125\xi^5$$

where

$$\xi = log_{10} k$$

Appendix AC

Solution of the Bateman Equations

Consider a chain of n radionuclides where N_1, N_2, N_3, N_d .....N_n represent the number of atoms of each of the radionuclides in the repository and where N_n is stable. The differential equations that govern the decay and growth are

$$\frac{dN_1}{dt} = -\lambda_1 N_1$$

$$\frac{dN_2}{dt} = \lambda_1 N_1 - \lambda_2 N_2$$

$$\frac{dN_3}{dt} = \lambda_2 N_2 - \lambda_3 N_3 \qquad (C1)$$

.....

.....

$$\frac{dN_n}{dt} = \lambda_{n-1} N_{n-1}$$

The initial number of atoms of radionuclide 1 in the repository is N_1^0 and the initial number of atoms of the daughter atoms are N_2^0, N_3^0, N_4^0 .....N_n^0. The disintegration constants are λ_1, λ_2, λ_3, λ_4 .....λ_{n-1} . The half lives of the radionuclides are related to the disintegration constants through the relation, $t_{\frac{1}{2}}$ =half life $= \frac{ln2}{\lambda}$.

The Laplace transform of N_i and $\frac{dN_i}{dt}$ will be defined by the notation (Hildebrand, 1962)

$$L\{N_i\} = f_i(s) \text{ and}$$

$$L\left\{\frac{dN_i}{dt}\right\} = sf_i(s) - N_i^0$$

Taking the Laplace transform of both sides of equations C1 results in

$$sf_1(s) - N_1^0 = -\lambda_1 f_1(s)$$
$$sf_2(s) - N_2^0 = \lambda_1 f_1(s) - \lambda_2 f_2(s)$$
$$sf_3(s) - N_3^0 = \lambda_2 f_2(s) - \lambda_3 f_3(s) \qquad (C2)$$

.....

.....

$$sf_n(s) - N_n^0 = \lambda_{n-1} f_{n-1}(s)$$

or solving for $f_1(s)$.....$f_n(s)$

$$f_1(s) = \frac{N_1^0}{s+\lambda_1}$$

$$f_2(s) = \frac{N_2^0 + \lambda_1 f_1(s)}{s+\lambda_2} = \frac{N_2^0}{s+\lambda_2} + \frac{\lambda_1 N_1^0}{(s+\lambda_1)(s+\lambda_2)}$$

$$f_3(s) = \frac{N_3^0 + \lambda_2 f_2(s)}{s+\lambda_3} = \frac{N_3^0}{s+\lambda_3} + \frac{\lambda_2 N_2^0}{(s+\lambda_2)(s+\lambda_3)} + \frac{\lambda_2\lambda_1 N_1^0}{(s+\lambda_1)(s+\lambda_2)(s+\lambda_3)}$$

..... (C3)

.....

$$f_n(s) = \frac{N_n^0}{s+\lambda_n} + \frac{\lambda_{n-1} N_{n-1}^0}{(s+\lambda_n)(s+\lambda_{n-1})} + \frac{\lambda_{n-1}\lambda_{n-2} N_{n-2}^0}{(s+\lambda_n)(s+\lambda_{n-1})(s+\lambda_{n-2})} + \ldots$$

$$. + \frac{\lambda_{n-1}\lambda_{n-2}\ldots.\lambda_1 N_1^0}{(s+\lambda_n)(s+\lambda_{n-1})\ldots.(s+\lambda_1)}$$

The terms of equations (C3) can be rewritten in terms of partial fractions as

$$f_1(s) = \frac{N_1^0}{s+\lambda_1}$$

$$f_2(s) = \frac{N_2^0}{s+\lambda_2} + \frac{\lambda_1 N_1^0}{(s+\lambda_1)(\lambda_2-\lambda_1)} + \frac{\lambda_1 N_1^0}{(s+\lambda_2)(\lambda_1-\lambda_2)}$$

$$f_3(s) = \frac{N_3^0}{s+\lambda_3} + \frac{\lambda_2 N_2^0}{(s+\lambda_2)(\lambda_3-\lambda_2)} + \frac{\lambda_2 N_2^0}{(s+\lambda_3)(\lambda_2-\lambda_3)} +$$

$$+ \frac{\lambda_1\lambda_2 N_1}{(s+\lambda_1)(\lambda_2-\lambda_1)(\lambda_3-\lambda_1)} + \frac{\lambda_1\lambda_2 N_1}{(s+\lambda_2)(\lambda_3-\lambda_2)(\lambda_1-\lambda_2)}$$

$$+ \frac{\lambda_1\lambda_2 N_1}{(s+\lambda_3)(\lambda_1-\lambda_3)(\lambda_2-\lambda_3)} \quad \text{(C4)}$$

.....

.....

$$f_n(s) = \sum_{j=1}^{n} \frac{N_j}{(s+\lambda_n)} \prod_{i=j}^{n-1} \left(\frac{\lambda_i}{s+\lambda_i} \right)$$

Inverting equations (C4) back into the time domain obtains

$$N_1 = N_1^0 e^{-\lambda_1 t}$$

$$N_2 = N_2^0 e^{-\lambda_1 t} + \lambda_1 N_1^0 \left[\frac{e^{-\lambda_1 t}}{(\lambda_2 - \lambda_1)} + \frac{e^{-\lambda_2 t}}{(\lambda_1 - \lambda_2)} \right]$$

$$N_3 = N_3^0 e^{-\lambda_1 t} + \lambda_2 N_2^0 \left[\frac{e^{-\lambda_2 t}}{(\lambda_3 - \lambda_2)} + \frac{e^{-\lambda_3 t}}{(\lambda_2 - \lambda_3)} \right]$$

$$+ \lambda_1 \lambda_2 N_1^0 \left[\frac{e^{-\lambda_1 t}}{(\lambda_2 - \lambda_1)(\lambda_3 - \lambda_1)} + \frac{e^{-\lambda_2 t}}{(\lambda_3 - \lambda_2)(\lambda_1 - \lambda_2)} + \frac{e^{-\lambda_3 t}}{(\lambda_1 - \lambda_3)(\lambda_2 - \lambda_3)} \right] .$$

.....

.....

$$N_n = \sum_{j=1}^{n} N_j^0 \prod_{i=j}^{n-1} \lambda_i \sum_{i=j}^{n} \left(\prod_{l=j+1}^{n} \frac{1}{\lambda_l - \lambda_i} \right) e^{-\lambda_i t}$$

Appendix AD
Parting Stress Based on Pore Water

Consider two spherical particles in contact with a small volume of liquid surrounding the point of contact (Figure D1). Assume that the surface tension is T and the pressure within the liquid is P_c and outside the liquid is P_o. For static equilibrium of a small element of the liquid surface

$$(P_c - P_o)ds'ds'' + 2T\sin\left(\frac{d\theta'}{2}\right)ds'' - 2T\sin\left(\frac{d\theta''}{2}\right)ds' = 0 \qquad \text{(D1)}$$

or

$$(P_c - P_o)ds'ds'' + 2T\left(\frac{d\theta'}{2}\right)ds'' - 2T\left(\frac{d\theta''}{2}\right)ds' = 0 \qquad \text{(D2)}$$

thus

$$(P_c - P_o)ds'ds'' + Td\theta'ds'' - Td\theta''ds' = 0 \qquad \text{(D3)}$$

but

$ds' = r'd\theta'$ and $ds'' = r''d\theta''$

Therefore

$$P_c - P_o = T\left(\frac{1}{r''} - \frac{1}{r'}\right) \qquad \text{(D4)}$$

The quantity $P_c - P_o$ represents the capillary pressure in the liquid volume. To physically separate the two spherical particles requires a force F

$$F = 2\pi r''T - (P_c - P_o)\pi r''^2 \qquad \text{(D5)}$$

The parting stress is based on the projected area of a particle and the force F. It can be written

$$\sigma_p = \frac{F}{\pi R^2} = \frac{2\pi r''T - (P_c - P_o)\pi r''^2}{\pi R^2} = \frac{2r'T - T\left(\frac{1}{r''} - \frac{1}{r'}\right)r''^2}{R^2} \qquad \text{(D6)}$$

where from geometry (Figure D2)

$$r'' = -r' + \sqrt{r'^2 + 2r'R} \qquad \text{(D7)}$$

The above analysis assumes that only one fluid contact point is involved in the determination of the parting stress. For more densely packed material as many as three fluid contact points should be considered resulting in a greater stress. However to be conservative only one fluid contact point is assumed.

Waste Saturation

The volume of liquid associated with each particle contact is

$$V_w = 2\pi w^2 h - 2V_R - V_c \qquad \text{(D8)}$$

Where V_R is the volume associated with a portion of the particle formed by a plane passing through the particle a distance h from the particle surface, and V_c is the toroidal volume defined by an area A rotated around axis a'. The area of the latter is delineated by the straight line 2h and a portion of the circle of radius r' (Figure D3).

$$V_R = \frac{1}{3}\pi h^2(3R - h) \qquad \text{(D9)}$$

$$V_c = 2\pi A\left[r'' + r' - \frac{2r'}{3}\left(\frac{\sin^3\theta}{\theta - \sin\theta\cos\theta}\right)\right] \qquad \text{(D10)}$$

where

$$A = \frac{r'^2}{2}(2\theta - \sin 2\theta) \qquad \text{(D11)}$$

The liquid saturation is defined as the ratio of the liquid volume to the total void volume in a sample of material. Void volume is a function of particle shape, particle size distribution, and packing density. For spherical particles of a single diameter the maximum percent voids (void ratio) is 37.5% (Katz, HS, et al 1978). The number of single size particles (N) within a volume (V) of material at maximum packing density is

$$N = \frac{(1 - 0.375)V}{\frac{4}{3}\pi R^3} \qquad \text{(D12)}$$

Within the volume V each particle is in contact with 12 surrounding particles. Thus the volume of liquid associated with N particles is

$$V_{wt} = 6V_w N \qquad \text{(D13)}$$

And the saturation (S) is

$$S = \frac{V_{wt}}{0.375V} \qquad \text{(D14)}$$

or

$$S = 2.39\frac{V_w}{R^3} \qquad \text{(D15)}$$

For a known saturation S and particle radius R it is possible to back solve for r' and the parting stress σ_p. This must be done numerically because of the complexity of the governing equations. Using equation (D8) and (D15) a variable Q can be defined thus

$$Q = V_w - \frac{SR^3}{2.39} = 2\pi w^2 h - 2V_R - V_c - \frac{SR^3}{2.39} = 0 \qquad \text{(D16)}$$

The iterative numerical procedure used to determine the value of r' that satisfies equation (D16) is illustrated in Figure D4. The value of r' from the solution of equation (D16) can then be used to determine the parting stress using equations (D6) and (D7). The parting stress can then be used to compute the effective acceleration of gravity utilizing equation (37a).

Strength effects arising from moisture content of the waste can thus be included in the blowout model utilizing the waste saturation at the time of intrusion and the assumed waste particle radius. The waste particle radius is an unknown quantity which will have to be sampled.

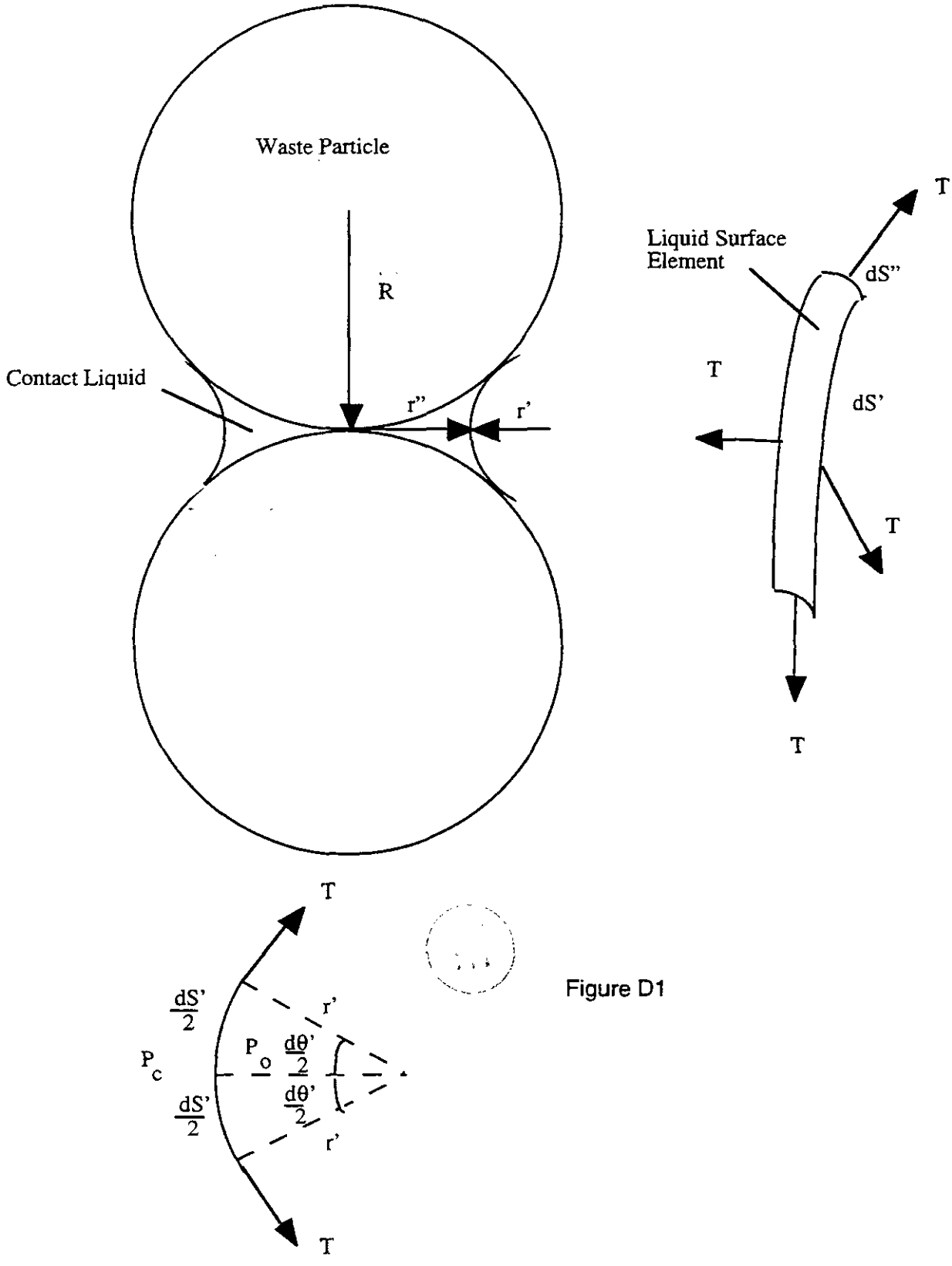
Waste Particle
R
Contact Liquid
r"
r'
Liquid Surface
Element
dS"
dS'
T
T
T
T
T
dS'/2
r'
P_o
dθ'/2
P_c
dθ'/2
dS'/2
r'
T

Figure D1

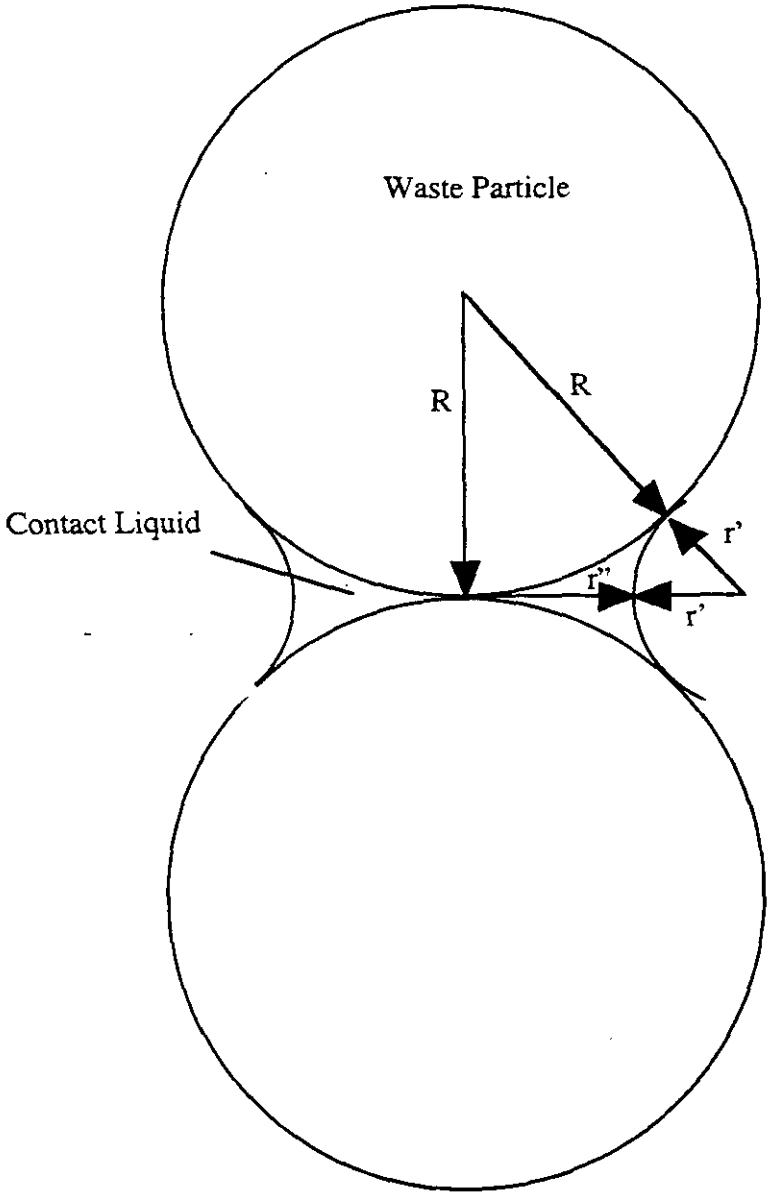

Figure D2

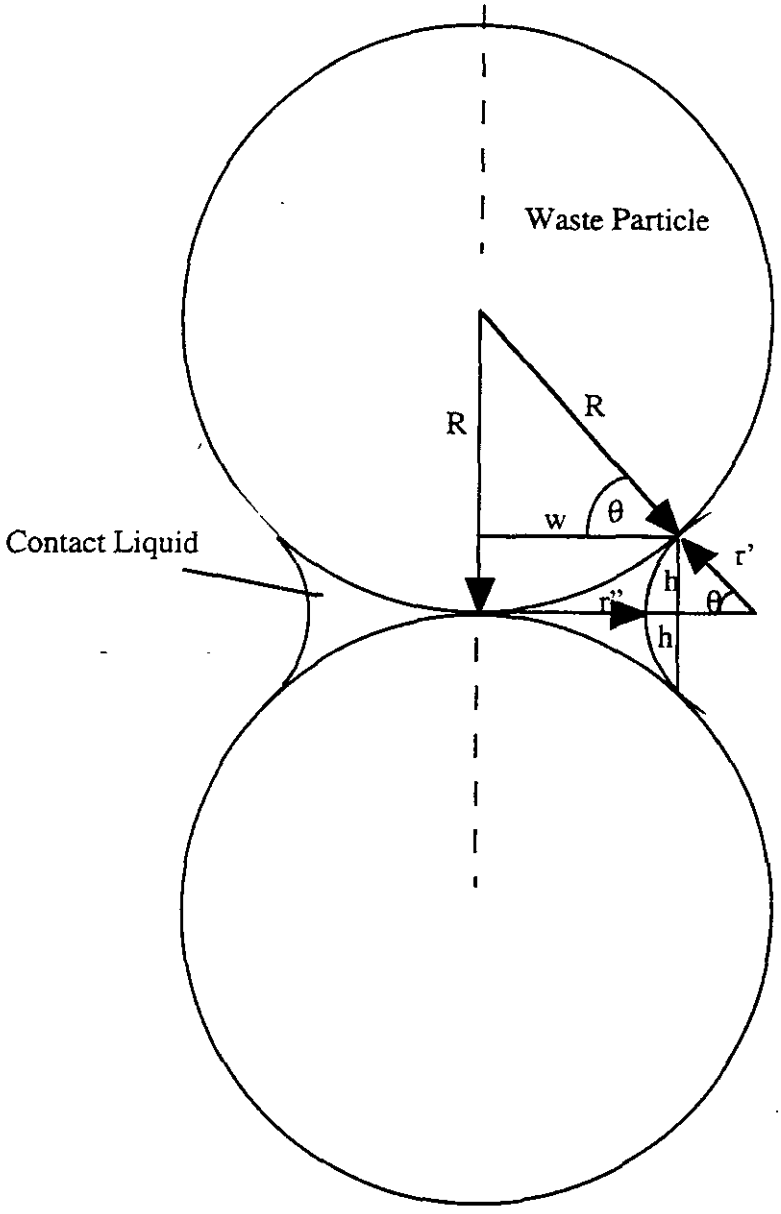

Figure D3

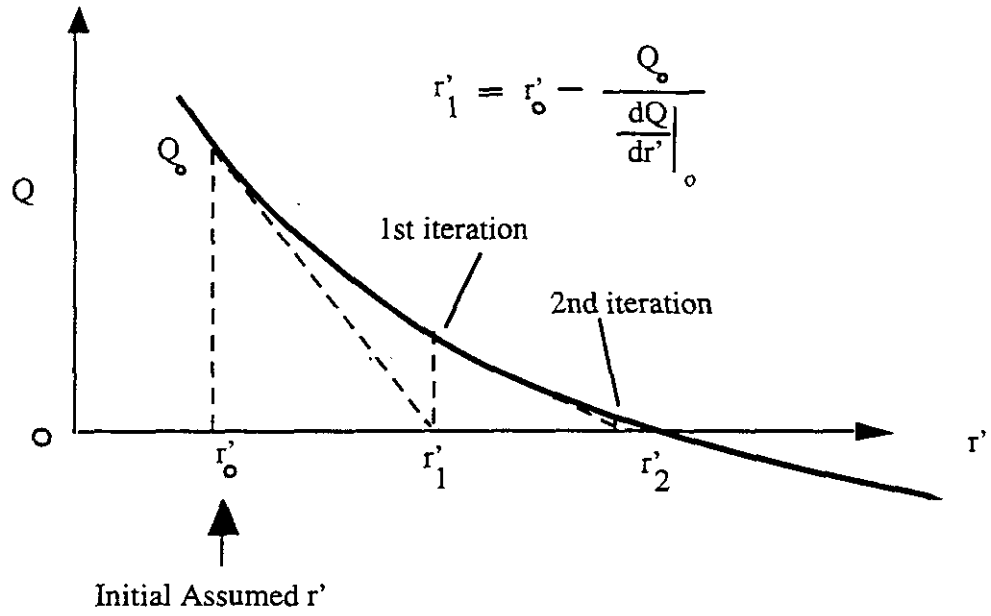
$r'_1 = r'_o - \frac{Q_o}{\left.\frac{dQ}{dr'}\right|_o}$
Q_o
Q
1st iteration
2nd iteration
o
r'
r'_o
r'_1
r'_2
Initial Assumed r'

Figure D4

References

Austin, E.H., 1983, *Drilling Engineering Handbook*, International Human Resources Development Corporation, Boston, p78.

Berglund, J.W., 1993, *Mechanisms Governing the Direct Removal of Wastes from the WIPP Repository Caused by Exploratory Drilling,* SAND-92-7295, Sandia National Laboratories, Albuquerque, NM.

Berglund, J.W., 1994, *The Direct Removal of Waste Caused by a Drilling Intrusion Into a WIPP Panel ---A Position Paper,* Memorandum of Record, 31 August 1994

Bilgen E., Boulos, R., and Akgungor A.C., 1973, "Leakage and Frictional Characteristics of Turbulent Helical Flow In Fine Clearance, "*Journal of Fluids Engineering*, Volume 95, pp 493-497.

Binder . R.C., 1958, *Advanced Fluid Mechanics Volume 1*, Prentice Hall, Inc. Englewood Cliffs N.J. p. 63.

Broc, R., ed. 1982. *Drilling Mud and Cement Slurry Rheology Manual.*, Houston, TX: Gulf Publishing Company.

Cheremisinoff, N. P., and P. N. Cheremisinoff, 1984, *Hydrodynamics of Gas-Solids Fluidization,* Gulf Publishing Company, Houston p 30.

Coleman, B.D., and W. Noll. 1959. "Helical Flow of General Fluids," *Journal of Applied Physics.* Vol. 30, no. 10, 1508-1515.

Darley, H.C.H., and G.R. Gray. 1988. *Composition and Properties of Drilling and Completion Fluids.* Houston, TX: Gulf Publishing Company.

Fox, R. W., and McDonald, A. T., 1973, *Introduction to Fluid Mechanics*, John Wiley and Sons, New York, p 406.

Fredrickson, A.G. 1960. "Helical Flow of an Annular Mass of Visco-Elastic Fluid," *Chemical Engineering Science.* Vol. 11, no. 3, 252-259.

GASFLOW---Code to Compute Gas Flow in a Porous Medium. (Since Model 1 for spall will not be used for performance assessment, this code has not been formally documented)

Hildebrand, F.B., 1962, *Advanced Calculus for Applications*, Prentice Hall, Englewood Cliffs NJ, p53.

Kaplan, I., 1962, *Nuclear Physics*, Addison-Wesley, Reading Massachusetts, p242.

Katz H.S. and Milewski, J.V., Ed., 1978, *Handbook of Fillers and Reinforcements for Plastics*, Van Nostrand Reinhold, New York, p68.

Khader, M.H.A., and H.S. Rao, 1974, "Flow Through Annulus with Large Radial Clearance," *Proceedings of the American Society of Civil Engineers, Journal of the Hydraulics Division,* HY1, January, 1974.

Lenke, L.R., Berglund, J.W., and Cole R. A., March 1996, *Blowout Experiments using Fine Grained Silica Sands in an Axisymmetric Geometry,* Contractor Report 1996/7/32250, New Mexico Engineering Research Institute, University of New Mexico.

Marquis, J., September 22, 1995. Memorandum of Record SWCF-A:1.1.1.2.7:PA:QA: Summary of Gas/Oil Well Drill Collar Size Survey

Obert, E.F., *Thermodynamics,* McGraw- Hill, New York 1948, Table VI page 541.

Oldroyd, J.G., 1958, *Proceedings of the Royal Society (London),* A245, p. 278.

Parthenaides, E, and R.E. Paaswell, 1970, "Erodibility of Channels with Cohesive Boundary," *Proceedings of the American Society of Civil Engineers, Journal of the Hydraulics Division,* 99: 555-558.

Rechard, R.P., H. Iuzzolino, and J.S. Sandha. 1990. *Data Used in Preliminary Performance Assessment of the Waste Isolation Pilot Plant (1990).* SAND89-2408. Albuquerque, NM: Sandia National Laboratories.

Salvadori, M.G., and M.L. Baron, 1961, Numerical Methods in Engineering, Prentice-Hall, Englewood Cliffs, N.J..

Sargunam, A., Riley, P., Arulanandan, K., Krone, R.B., 1973, "Physico-Chemical Factors in Erosion of Cohesive Soils", *Proceedings of the American Society of Civil Engineers, Journal of the Hydraulics Division* ,Vol.99, No. HY3, : 555-558, March 1973.

Savins, J.G., and G.C. Wallick. 1966. "Viscosity Profiles, Discharge Rates, Pressures, and Torques for a Rheologically Complex Fluid in a Helical Flow," *A.I.Ch.E. Journal.* Vol. 12, no. 2, 357-363.

Short, J.A., 1982, *Drilling and Casing Operations*, PennWell Books, Tulsa Oklahoma, p185.

Streeter, V.L., 1958, *Fluid Mechanics*, McGraw-Hill, New York.

Sandia WIPP Project. 1992 *Preliminary Performance Assessment for the Waste Isolation Pilot Plant, December 1992, Volume 3: Model Parameters,* Sandia Report SAND92-0700/3, Albuquerque NM, Sandia National Laboratories.

SNL Contract Document AL-7022, dated October 10,1994 - Period of Performance for this contract is 10/10/94 through 3/31/96.

Walker, R.E., 1976, "Hydraulic Limits are Set by Flow Restrictions", *Oil and Gas Journal*, October 4, 1976, pp 86-90.

Whittaker, A., 1985, Editor, *Theory and Application of Drilling Fluid Hydraulics*, (International Human Resources Development Corporation, Boston).